WIEN2k Hands-On Workshop for New and Existing Users | (SMR 3929)

08 Apr 2024 - 19 Apr 2024
ICTP, Trieste, Italy

P01 - ABBASNEJAD Mohaddeseh

First principles study of Ti-doped ZnO monolayer for NO gas sensing

P02 - ABDUR RASHID Mohammad

Analysis of structural, optoelectronic and elastic properties of lead-free cubic perovskite FrBX3 (B = Ca, Sr and X = Cl, Br, I): a first principle study

P03 - ADAK Abhishek Kumar

Self-assembled Magnetic Chain: Fe dimer coordinated Indigo Coordination Polymer on Au(111)

P04 - ALAY E ABBAS Syed Muhammad

Assessing the Performance of meta-GGAs for Bulk and 2D Modifications of Materials Exhibiting Non-Trivial Band Topologies: The Case of Anti-Pervoskite Ca3SnO

P05 - ALIKHAH Sanaz

Magneto-optical probing of orbital accumulation in a light metal

P06 - CAMARGO-MARTÍNEZ Jose Alfredo

First-principles calculations for structural, electronic, and phonon properties of H3S, D3S, MgB2 y Nb-bcc conventional superconductors under pressure

P07 - CHRAFIH Younes

Thermodynamic, optical, and morphological studies of the Cs2AgBiX6 double perovskites (X = Cl, Br, and I): Insights from DFT study

P08 - DEMCHENKO Iraida

Effects of Si/N Ion Implantation on Defect formation and Doping of Gallium Oxide

P09 - DORJ Sodkhuu

Iron-based permanent magnet materials design

P10 - DUTT Rajeev

Role of isovalent substitution in band-convergence and thermoelectric properties of chalcogen based half-Heusler alloys

P11 - EL HAJ HASSAN Fouad

Structural, electronic, optical and thermal properties of Ga2O3 polymorphs

P12 - EL OUARIE Nassima

Unraveling the Power of CNGS-Based Kesterite Solar Cells through Cutting-Edge DFT and SCAPS-1D Analysis

P13 - FECHTELKORD Michael Franz

Cation and anion ordering in synthetic lepidolites and lithian muscovites: Influence of the OH/F and Li/Al ratios on the mica formation studied by NMR spectroscopy and X-ray diffraction

P14 - GHOSH Anima

Computational Investigation on Electronic Properties of Inorganic Chalcogenide Solar Absorber Material

P15 - HUSAIN Munavvar

Quantum Chemistry Topology methods for excited states. A pilot study using Benzene

P16 - KHAN Saleem Ayaz

Influence of Hf (0001) surface contamination on ARPES: a DFT study supporting experiments

P17 - KOCHUMANNIL VARGHESE Jovan Jose

A Graph Neural Network-based Algorithm for Global Optimization of Atomic Clusters

P18 - KUMAR Nilesh

Computational Insights into Exciton Radiative Lifetimes in Hf-Based MXenes by many-body methods.

P19 - MAHAMIYA Vikram

Influence of defects on the structural, electronic, and optical properties of 2D-SiC and MoS2.

P20 - MAHRAJ Issam

First-principles investigations of structural and electronic properties of ternary chalcopyrite semiconductors $uInY_2$ ($Y = S$, Se and Te).

P21 - MOSTAFAEI Alireza

Tight-binding model for the electronic structure of Lu2CF2 2D MXene based on the WIEN2k calculation

P22 - NANDI Pranjal

Investigation of local dielectric function of HfO2 thin layers with different crystallographic phases by EELS Analysis and DFT Simulations.

P23 - PANDEY Dhanshree

An investigation of the W-Ta-Vacancy system: A combined DFT and Cluster expansion study

P24 - PANDEY Vivek

PY-Nodes: An ab-initio python code for searching nodes in a material using Nelder-Mead's simplex approach.

P25 - PATEL Saurav

Topological Insulating Phase in Non-centrosymmetric LiSrBi Compound

P26 - PAWELKO Jakub

Computational modelling of all-solid state batteries containing Li2S-P2S5 glasses as an electrolyte

P27 - RAHIMI Shahrbano

Nonzero spontaneous electric polarization in metals: Novel predictive methods and applications

P28 - RAKSHIT Subrata

The structure and properties of Bilayer Borophene

P29 - ROZALE Habib

Dopants effect on the electronic and catalysis properties of Silver oxides: DFT

P30 - SANGEETA -

Thermoelectric Performance of Li-based Half-Heusler Alloys: A First-Principles Investigation

P31 - SHAN Guangcun

Novel two-dimensional room-temperature ferromagnetic layered GdB2N2 material with large perpendicular magnetic anisotropy

P32 - SILVA DE SOUSA Pedro Alexandre

Ab-initio Study on CsNdNb2O7 and CsLaNb2O7 Dion-Jacobson Perovskites

P33 - SMOLYANYUK Andriy

AMcheck: a tool to check whether a symmetry-compensated collinear magnetic material is antiferro- or altermagnetic

P34 - TUMENTSEREG Ochirkhuyag

Magnetism and magnetic anisotropy of a single rare-earth atom on transition metal dichalcogenides: A first-principles prediction

P35 - VAIDYANATHAN Antara

Interaction mechanism of rare earths with γ-Graphyne: Comparative analysis using an all-electron and pseudoelectron-based DFT approach

P36 - VASILYEV Dmitry

First-principles phonon calculations of thermal expansion path of Fe2Mo Laves phase

P37 - YADAV Anita

Inducing out-of-plane magnetocrystalline anisotropy by chemical doping in 2D multiferroic CuCrP2S6.

P38 - GOMEZ Andres

Elucidating the chemical and structural variability in the efficiency of band edge optical transitions of 2D monolayer materials

First principles study of Ti-doped ZnO monolayer for NO gas sensing

Z. Mahmoudi Gushkin [1] , R. Maezono [2] , M. Abbasnejad [1]

[1] *Faculty of Physics, Shahid Bahonar University of Kerman, Kerman, Iran*
[2] *School of Information Science, JAIST, Asahidai 1-1, Nomi, Ishikawa 923-1292, Japan*

The ZnO monolayer is a new graphene-like material with interesting electronic and magnetic properties, along with sufficient chemical stability [1]. Graphene-like ZnO was reported to be a typical n type semiconductor with an inherent band gap. The density of the carriers (mainly electrons) in graphene-like ZnO has been effectively modified with the adsorption of gas molecules and successfully applied in the field of gas sensors. NO is a harmful gas produced from burning traditional fossil fuels [2]. High-centration NO can do significant harm when introduced into the human body. As a result, it is of great importance to use a sensing material to adsorb or sense the NO. Here, we would like to investigate the adsorption of the NO molecule onto a pure ZnO monolayer and ZnO modified with a Ti atom within the framework of density functional theory. The main goal of this work is proposing a good material for gas sensing and improving the its performance by selecting proper dopant.

[1] U. Özgür, *et al.*, J. Appl. Phys. **98**, 041301 (2005).
[2] M. Breedon, M. J. S. Spencer, and I. Yarovsky, Surf. Sci. **603**, 3389 (2009).

Analysis of structural, optoelectronic and elastic properties of lead-free cubic perovskite FrBX$_3$ (B = Ca, Sr and X = Cl, Br, I): a first principle study

Mohammad Abdur Rashid[1], **Md. Borhanul Asfia**[1], **and Sahadat Jaman**[1]

[1]*Quantum Materials Simulation Lab (QMSL), Department of Physics, Jashore University of Science and Technology, Jashore 7408, Bangladesh*

Perovskites made of inorganic halide have a wide range of uses in cost effective photovoltaic and optoelectronic systems. In this investigation, density functional theory was used to determine the structural, elastic, electronic and optical characteristics of pristine lead-free perovskites FrBX$_3$ (B = Ca, Sr and X = Cl, Br, I). This samples showed semiconducting activity with indirect bandgap energy and mechanical phase consistency. The replacements of cations and anions sitting over the B and X sites of the FrBX$_3$ molecule explain the observed fluctuation in the bandgap. From the calculation it is noticed that the bandgap is decreased when Ca is substituted by Sr in B site of FrBX$_3$ (X = Cl, Br, I). These materials are useful for photovoltaic and other optoelectronic device applications because of their high absorption coefficient, low reflection and strong optical conductivity. Mechanical properties of FrBX$_3$ are indicated that except FrCaCl$_3$ and FrCaBr$_3$, all other compounds are ductile in nature. FrBX$_3$, a perovskite containing the radioactive element Fr, might have uses in nuclear medicine and treatment.

Self-assembled Magnetic Chain: Fe dimer coordinated Indigo Coordination Polymer on Au(111)

A. K. Adak[1,2], H. Xu[3], B. Yang[3], D. Meier[3], A. Riss[3], J. Reichert[3], S. Narasimhan[2], J. V. Barth[3], A. C. Papageorgiou[3,4]

[1] Abdus Salam International Centre for Theoretical Physics (ICTP)

[2] Jawaharlal Nehru Centre for Advanced Scientific Research (JNCASR)

[3] Technical University of Munich (TUM)

[4] National and Kapodistrian University of Athens

Coordination polymers represent promising prospects for miniaturized electronics, offering unconventional electronic and magnetic traits that make them appealing for various applications, including magnetic information storage devices to spintronics. Harnessing natural products for material tailoring presents inherent advantages in biodegradation. Among these, indigo, a historic natural dye renowned for its distinctive blue hue, has captivated attention due to its optical properties and the formation of various metal complexes.[1] Herein, we utilize indigo as a molecular building block to fabricate a surface-bound coordination polymer with iron (Fe), capitalizing on the unique properties of magnetic nanoparticles, keeping in mind its vast applications ranging from targeted drug delivery to magnetic resonance imaging and spintronics.

Through a collaborative experimental and theoretical endeavor, we explore the formation and characteristics of a one-dimensional (1D) indigo coordination polymer on an Au(111) metal substrate, featuring double Fe coordination. Termed a "1D magnetic chain," this polymer incorporates Fe cation centers exhibiting magnetic properties, with each pair of neighboring indigo molecules hosting a dimer of two Fe adatoms. Detailed Density Functional Theory (DFT) analyses shed light on the structural, electronic, and magnetic attributes of this system. Our investigations reveal that altering the relative orientation of magnetic moments within Fe dimers significantly impacts both the DFT-calculated total energy and structural properties of the magnetic chain. Conversely, modifying the orientation between neighboring dimers exerts minimal influence on the system's structural and electronic characteristics, suggesting the quasi-independence of dimers as magnetic centers. The fact that the dimers are essentially acting as independent magnetic centers may result in making the 1D magnetic chain an ideal candidate for magnetic memory storage applications.

This study serves as an exemplary model for understanding 1D magnetic chains, offering profound implications for magnetic memory storage devices. Furthermore, it provides valuable insights into the manipulation and engineering of magnetic nanoparticles, particularly Fe atoms organized into compact clusters, facilitating further refinement and exploration of their magnetic properties.

[1]   W. Beck, K. Sünkel, *Z. Anorg. Allg. Chem.* **2020**, *646*, 248-255.

Abstract for Poster Session

Assessing the Performance of meta-GGAs for Bulk and 2D Modifications of Materials Exhibiting Non-Trivial Band Topologies: The Case of Anti-Pervoskite Ca$_3$SnO

Syed Muhammad Alay-e-Abbas [1,2], Ghulam Abbas [1], Waqas Zulfiqar [2,3], Muhammad Sajjad [1,4], Nirpendra Singh [4,5] and J. Andreas Larsson [1]

[1] *Applied Physics, Division of Materials Science, Department of Engineering Sciences and Mathematics, Luleå University of Technology, 97187, Luleå, Sweden*

[2] *Computational Materials Modeling Laboratory, Department of Physics, Government College University, Faisalabad, 38040, Pakistan*

[3] *Department of Energy Conversion and Storage, Technical University of Denmark, 2800, Kgs. Lyngby, Denmark*

[4] *Department of Physics, Khalifa University of Science and Technology, Abu Dhabi, 127788, United Arab Emirates*

[5] *Center for Catalysis and Separation (CeCaS), Khalifa University of Science and Technology, Abu Dhabi, 127788, United Arab Emirates*

The non-trivial band topplogies of anti-perovskite Ca$_3$SnO find their origin in the intricate competition between band overlap, spin-orbit coupling and crystal symmetry. While the bulk properties of this material have been extensively explored both theoretically and exprimentally [1, 2], the properties of one unit cell thick 2D monolayer of anti-perovskites Ca$_3$SnO are unexplored. The recent progresses in synthesizing freestanding 2D perovskite oxides monolayers [3] makes it intuitive to theoretically explore the physical properties of anti-perovskite monolayers whose bulk modofications exhibit non-trivial band topologies. Motivated by this, we have carried out a comaprison of the structural, thermodynamic, electronic, and thermoelectric properties of bulk and monolayer anti-perovskite Ca$_3$SnO by employing dispersion-corrected SCAN+rVV10 and mBJ/lmBJ meta-GGA functionals of DFT [4]. After confirming the performance of these meta-GGA functionals in reproducing exprimentally obsrved thermoelectric properties of bulk Ca$_3$SnO, we deploy the same set of meta-GGAs to predict properties of 2D Ca$_3$SnO monolayer. Our results show that Rashba-type splitting in the electronic structure of 2D Ca$_3$SnO monolayer originating from the presence of strong spin-orbit coupling and absence of inversion symmetry enhances its thermoelectric properties compared to bulk Ca$_3$SnO [4].

1. T.H. Hsieh, J. Liu, L. Fu, Phys. Rev. B. **90**, 81112 (2014).
2. Y. Okamoto, A. Sakamaki, K. Takenaka, J. Appl. Phys. **119**, 205106 (2016).
3. D. X. Ji, S. H. Cai, T. R. Paudel, H. Y. Sun, et al. Nature 570, 87–90 (2019).
4. S.M. Alay-e-Abbas, G. Abbas, W. Zulfiqar, M. Sajjad, N. Singh, J. A. Larsson, Nano Res. 16, 1779 (2023).

Magneto-optical probing of orbital accumulation in a light metal

<u>Sanaz Alikhah</u> [1] , Marco Berritta[2] , Peter M. Oppeneer[1], Igor Lyalin[3], and Roland K. Kawakami[3]

[1] *Uppsala University, Uppsala, Sweden*
[2] *University of Exeter, Exeter, United Kingdom*
[3]*Ohio State University, Ohio, USA*

Orbital currents and orbital accumulation are attractive alternatives to the commonly employed spin counterparts, generated typically by the spin Hall effect in heavy-metals. However, the detection of orbital currents and accumulation is a challenging task. Here we investigate theoretically the possibility of magneto-optical (MO) detection of current-induced orbital accumulation in the light metal chromium. Using linear-response theory, we compute first the spin and orbital accumulation and then predict the expected MO spectrum for pure spin accumulation or pure orbital accumulation. We find that the orbital Hall effect is much larger than the spin Hall effect, and that the orbital MO response is much larger than that due to the spin polarization. This result opens the door for MO detection of current-induced orbital accumulation. Finally, we compare the computed MO responses with recent MO Kerr effect measurements on chromium.

First-principles calculations for structural, electronic, and phonon properties of H_3S, D_3S, MgB_2 y Nb-bcc conventional superconductors under pressure

J. A. Camargo Martínez [1] and H. H. Chinome-Alba [1]

[1]*(PhD in physics, theoretical solid-state physics) Grupo de Investigación en Ciencias Básicas, Aplicación e innovación- CIBAIN, Unitrópico, Yopal, Colombia*

In this work, we investigated the structural, electronic and phonon properties of H_3S, D_3S, MgB_2 y Nb-bcc conventional superconductors using density functional theory (DFT) as implemented in the WIEN2k code. Our interest is focused on evaluating the effect of pressure on the electronic and phononic properties of some well-known superconducting compounds, with the idea of establishing possible correlations with observed patterns in the functional derivative of Tc with respect to the electron-phonon spectral function $\alpha^2 F(\omega)$, $\delta Tc/\delta\alpha^2 F(\omega)$, as a function of Tc and pressure. These patterns have already been reported in the literature [1] and appear to have some relationship with the superconducting temperature Tc measured in these systems. This study aims to establish a potential mechanism for a Tc prediction based on the $\delta Tc/\delta\alpha 2F(\omega)$.

[1] Camargo-Martínez J, Mesa F, González-Pedreros G (2023) Temperature effects on the calculation of the functional derivative of Tc with respect to $\alpha 2F(\omega)$. PLoS ONE **18(6)**: e0286855. https://doi.org/10.1371/journal.pone.0286855

Thermodynamic, optical, and morphological studies of the Cs_2AgBiX_6 double perovskites (X = Cl, Br, and I): Insights from DFT study

<u>Younes chrafih</u>[1,*], Mohamed Al-Hattab[2,3], Khalid Rahmani[1, 2, 3]

[1]*Lphe-modeling and simulation Faculty of Science, Mohammed V University in Rabat, Moroccco,*

[2]*Research Laboratory in Physics and Sciences for Engineers (LRPSI), Poly-disciplinary Faculty, Sultan Moulay Slimane University, Beni Mellal, Morocco,*

[3]*Ecole Normale Supérieure (ENS), Mohammed V University, in Rabat, Morocco.*

In contrast to Pb-based perovskites, Cs_2AgBiX_6 (X = Cl, Br, I) double silver-bismuth perovskites have unveiled a promising future for the advancement of low-risk solar energy due to their high durability and non-toxicity of their constituents. Despite the focus on the optoelectronic properties of Cs_2AgBiX_6 double perovskites, research into their structural properties behavior has been limited. So in this paper, we investigated in depth the cubic structure of Cs_2AgBiX_6 double perovskites. The newly acquired cubic phase is more in line with current experimental results in optoelectronic characteristics, exhibiting higher optical properties useful for optoelectronic device design. All three halide compounds exhibit an indirect band gap character due to the highly dispersive nature of the valence band maximum and conduction band minimum, resulting in reduced effective mass values, as well as the disordering of the Ag^+ and Bi^{3+} cations in their sublattices. The thermodynamic potentials of phonon modes include enthalpy (H), free energy (F), entropy (S), and heat capacity (C). The optical and thermodynamic properties of pure $Cs_2AgBiCl_6$ and $Cs_2AgBiBr_6$ samples imply that they have promising qualities for optoelectronic and photovoltaic applications.

[1] W.S. Yang, B.W. Park, E.H. Jung, N.J. Jeon, Y.C. Kim, D.U. Lee, S.S. Shin, J. Seo, E.K. Kim, J.H. Noh, S. Il Seok, Iodide management in formamidinium-lead-halide- based perovskite layers for efficient solar cells, Science 356 (2017) 1376–1379, https://doi.org/10.1126/science.aan2301

[2] P. Docampo, J.M. Ball, M. Darwich, G.E. Eperon, H.J. Snaith, Efficient organometal trihalide perovskite planar-heterojunction solar cells on flexible polymer substrates, Nat. Commun. 4 (2013) 1–6, https://doi.org/10.1038/ncomms3761

Effects of Si/N Ion Implantation on Defect formation and Doping of Gallium Oxide

Iron-based permanent magnet materials design

D. Sodkhuu[1,2], N. Otgonzul[1], T. Tsevelmaa[1], N. Tsogbadrakh[1,*], B. Khongorzul[2], E. Uyanga[2], N. Jargalan[2], D. Sangaa[2], N. Batnyam[3,4], D. Odkhuu[2,3,4], and Kh. Odbadrakh[5]

[1]Department of Physics, National University of Mongolia, Ulaanbaatar 14201, Mongolia

[2]Institute of Physics and Technology, Mongolian Academy of Sciences, Ulaanbaatar 13330, Mongolia

[3]School of Applied Sciences, Mongolian University of Science and Technology, Ulaanbaatar 14191, Mongolia

[4]Department of Physics, Incheon National University, Incheon 22012, South Korea

[5]National Institute for Computational Sciences, Oak Ridge, TN 37996, USA

Since neodymium–iron–boron ($Nd_2Fe_{14}B$) permanent magnet was developed in 1985 (J. Appl. Phys. 57, 4094 (1985)), a permanent magnet with higher performance has not been reported yet. Ever since, search for permanent magnet materials that do not contain rare-earth elements, but compatible to ferrites in price, is underway. In this poster presentation, we will review the properties that make a material good permanent magnet, including saturation magnetization, uniaxial magnetocrystalline anisotropy, maximum energy density product, Curie temperature, and thermodynamic stability and discuss our approach to designing new permanent magnets free or reduced content of rare-earth elements while retaining a comparable performance with $Nd_2Fe_{14}B$. In addition, preliminary results of our density-functional theory calculations, implemented in WIEN2k, through the collaborations with our collaborators at the Incheon National University, South Korea, and Oak Ridge National Laboratory, USA, for the selected Fe–Sm–N, Fe–Co–P, and Fe–Ni–Ga alloys, will be presented. These results will also be discussed in comparison with experimental results done by our research colleagues at the Institute of Physics and Technology, Mongolian Academy of Sciences.

*N. Tsogbadrakh, Department of Physics, School of Arts and Sciences, National University of Mongolia, Ulaanbaatar 14201, Mongolia; Email: Tsogbadrakh@num.edu.mn; Tel: +97699647091

Role of isovalent substitution in band-convergence and thermoelectric properties of chalcogen based half-Heusler alloys

R. Dutt[1,2,3], **A. Chakrabarti**[2,3]

[1]*School of Engineering, Warwick University, CV47Al, United Kingdom,*
[2] *Homi Bhabha National Institute, Training School Complex, Anushakti Nagar, Mumbai400094, India*
[3] Theory and Simulations Laboratory, Human Resources Development Section, Raja Ramanna Centre for Advanced Technology, Indore452013, India

In this work, we have probed the 18 valence electrton (VEC) based half Heusler chalcogenides (HHC) with stoichiometry AXZ, where chalcogens(ns^2np^4) are placed at Z@(0, 0, 0) sites, with A@(0.25, 0.25, 0.25) and X@(0.5, 0.5, 0.5) sites occupied by d-block elements from first and seventh columns to maintain a total of 18 VEC. In order to check the possibilities of the experimental synthesis of these alloys, we have systematically investigated the probed alloys' energetic, mechanical, dynamical, and chemical stability.

A detailed analysis of the electronic structure of the probed alloys reveals that valence band maxima (VBM) shifts from high symmetry Γ(single-fold) to L(six-fold) with the increase in the atomic mass at the A site. In contrast, substituting elements with higher atomic mass at the X site increases the energy corresponding to the valence bands at high symmetry Γ point. Further, we found that use of exchange-correlation (XC) based on generalized gradient approximation undermines the band-gap values and more importantly sometiimes lead to incorrect band dispersion.

Further, we found that owing to the high value of valley degeneracy (N_V) in the valence band, the power factor of YCoC(C= S, Se, Te) and LaCoC(C= S, Se, Te) alloys for p-type doping is more than the 100% and 80%, respectively compared to the well known TiNiSn alloy. Further, the presence of high N_V in the conduction regime leads to similar enhancement in the case of ScCoTe, YCoTe, and ScRhTe. Besides the power factor, as discussed before value of thermal conductivity is crucial for the ZT values. Most of the HHCs possess the intermixing of the acoustical and optical phonons (except ScCoTe), which led to lowering of thermal conductivity. As a consequence, all of the probed HHCs show a significant improvement in the values of ZT as compared to the TiNiSn. So, we conclude here that HHCs with and without doping are worth-studying systems for their potential for TE applications.

[1] *Investigation of mechanical, lattice dynamical, electronic and thermoelectric properties of half heusler chalcogenides: a DFT study*, **R. Dutt**, J. Bhattacharya, A. Chakrabarti, J. Phys. Chem. Solids **167**, 110704 (2022).

Structural, electronic, optical and thermal properties of Ga_2O_3 polymorphs

Fatima Safieddine[a,b], Fouad El Haj Hassan[a,c]

[a]Platform for Research and Analysis in Environmental Sciences (PRASE-DSST), Campus Rafic Hariri, Lebanese University, Beirut, Lebanon
[b]Department of Physics, American University of Beirut, P.O. Box 11-0236, Riad El-Solh, Beirut 1107-2020, Lebanon
[c]Al Mlaaref University, Airport Avenue, Beirut, Lebanon

WIEN2k Hands-On Workshop for New and Existing Users, 08-19April 2024, Trieste, Italy

Abstract

We study the structural, electronic, elastic, optical, thermodynamic and transport properties of four different phases of Ga_2O_3 denoted by α, β, δ, and ε. The calculated gap energy E_g for the stable polymorph β-Ga_2O_3 is 4.6 eV which lies in the deep ultraviolet range making Ga_2O_3 promising for optoelectronics. Thermal effects on some macroscopic properties such as heat capacity, thermal expansion coefficient, Grüneisen parameter and Debye temperature are predicted using the quasi-harmonic Debye model. The analysis of transport properties for β-Ga_2O_3 using semi-classical Boltzmann transport theory in temperature range between 300 and 1000 K showed high Seebeck coefficient S=-348.4 μVK^{-1} at room temperature with huge power factor PF= 39.5×10^{10} WK^{-2}m^{-1}s^{-1} at T=1000 K. This suggests that Ga_2O_3 is a potential thermoelectric material.

Methods

Our calculations are done with the scalar relativistic FP-LAPW+lo method [1] within the framework of DFT as implemented in WIEN2K code. For electronic properties, after the structure optimization performed, the modified Becke-Johnson (mBJ) exchange potential was used, leading to improved band gap values [2].

Phase	α	β	δ	ε
Structure	Hexag.	Monocl.	cubic	Orthor.
Space group	R3c	C2/m	Ia3	Pna2$_1$
Point group	3m	2/m	m3	mm2
Atoms/unit cell	10	10	40	40
V/mole. (Å^3)	48.49	52.92	50.14	51.68
B(GPa)	221.08	199.29	212.30	207.68
B'	4.51	4.50	4.56	4.49

α-Ga_2O_3 β-Ga_2O_3 δ-Ga_2O_3 ε-Ga_2O_3
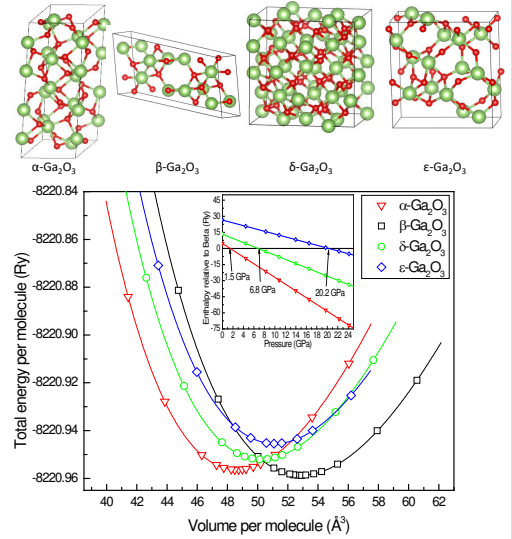
Introduction

The new technology urged semiconductor research to explore new materials with different band gaps. Researches started with Ge and Si to arrive at wide band gap (WBG) materials like SiC and GaN [3] which have (100-1000) times higher figure of merit (a quantity that characterizes effectiveness of a device relative to its alternatives) for power electronics than narrow band gap semiconductors, e.g., Si [3].

Gallium oxide later emerged as an alternative WBG material. Ga_2O_3 has the potential to perform well in future power electronics and optoelectronic applications at a much lower cost than SiC and GaN [4]. So, Gallium oxide has the future potential to be used as a transparent conducting oxide; it is electrically conductive, and it offers transparent windows from visible and UV light up to a wavelength of 250nm [5].

Phase	α-Ga_2O_3	β-Ga_2O_3	δ-Ga_2O_3	ε-Ga_2O_3
Young modulus (GPa)	312.018	344.477	296.891	329.391
Shear modulus (GPa)	123.107	142.271	117.203	130.232
Poisson ratio	0.267	0.210	0.266	0.264
Average velocity (m/s)	4872.09	5422.48	4833.48	5141.38
Debye temp. (K)	680.17	736.5	667.309	705.49
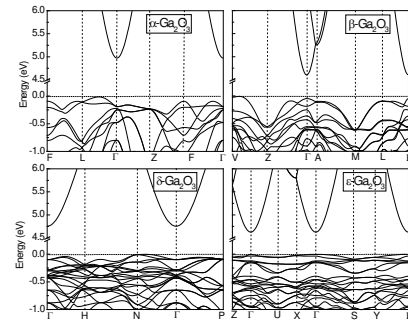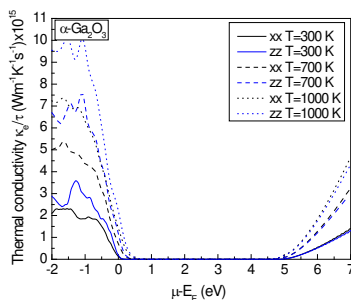
Phase	Gap character	Direct gap Γ mBJ (eV)	Indirect gap mBJ (eV)	Expt. eV [6]
α-Ga_2O_3	Indirect	5.164	4.987	4.99
β-Ga_2O_3	Indirect	4.690	4.593	4.60
δ-Ga_2O_3	Indirect	4.851	4.754	4.84
ε-Ga_2O_3	Direct	4.614	4.638	4.41
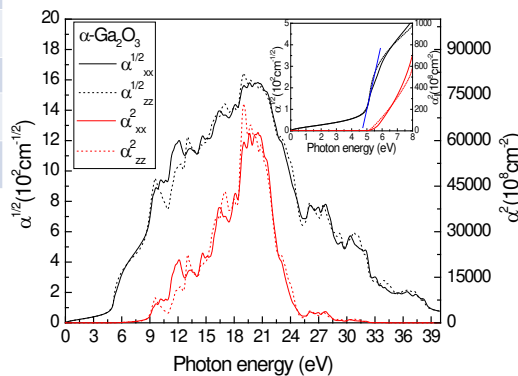
Results

The most thermodynamically stable monoclinic β-Ga_2O_3 phase at 1.5 GPa becomes outperformed by the rhombohedral α structure as the lowest-enthalpy one. Our calculations suggest that the α-Ga_2O_3 phase, in its turn, at 6.8 GPa becomes unstable against the δ phase. The δ to ε structural transformation is further on anticipated starting from 20.2 GPa.

α-Ga_2O_3, β-Ga_2O_3 and δ-Ga_2O_3 phases show an indirect band gap in the L-Γ, Z-V and N-Γ directions respectively, the ε phase shows a direct gap at Γ.

Thermal conductivity (k/τ) increases as the temperature T increases as shown the figure. The maximum value shown in zz-direction is 10.64×10^{15} (Wm^{-1}K^{-1}s^{-1}) at T=1000 K.

The maximum calculated figure of merit for the four phases at T=300 K is 0.997, meaning that gallium oxide is considered a promising high-performance thermoelectric material.

Conclusions

We studied the structural, electronic, optical, elastic, thermal, and transport properties of four different phases α, β, δ, and ε of gallium oxide (Ga_2O_3) using full potential linearized augmented plane wave method plus local orbitals within Density Functional Theory approximations. Calculations for all phases showed that Ga_2O_3 is an indirect wide band gap material with $E_g > 4.6$ eV and is considered as an ionic compound with a localized charge in the oxygen atom. The monoclinic phase (β-Ga_2O_3) was shown to be the most stable structure with the lowest enthalpy value. The optical properties were investigated and our results for the calculated dielectric function, reflectivity, and refractive index are in excellent agreement with experimental results. Finally, Transport properties revealed a high power factor and figure of merit making Ga_2O_3 a promising thermoelectric material.

Contact

Fouad EL HAJ HASSAN
EDST-PRASE, Lebanese University
hassan.f@ul.edu.lb
https://www.researchgate.net/profile/F-El-Haj-Hassan?ev=hdr_xprf
Phone: +961 3333814

References

1. K. Schwarz, P. Blaha, G.K.H. Madsen, Comput. Phys. Commun. 147 (2002) 71.
2. F. Tran, P. Blaha, J. Phys. Rev. Lett. 102 (2009) 226401. F. Tran, P. Blaha, J. Phys. Rev. Lett. 102 (2009) 226401.
3. M. Higashiwaki, S. Fujita, Gallium Oxide: Materials Properties, Crystal Growth, and Devices, Springer Nature, 293, 2020.
4. P.J. Wellmann, and Z. Anorg, Allg, Chem. 643 (2017) 1322.
5. R. A. Afre, N. Sharma, M. Sharon, Rev. Adv. Mater. Sci. 53 (2018) 89.
6. J. E. Swallow, C. Vorwerk, P. Mazzolini, P. Vogt, O. Bierwagen, A. Karg, M. Eickhoff, J. Schörmann, M. R. Wagner, J. W. Roberts, P. R Chalker, Chem. Mater. 32 (2020) 8470.

Unraveling the Power of CNGS-Based Kesterite Solar Cells through Cutting-Edge DFT and SCAPS-1D Analysis

N. El Ouarie [1,2], J. El Hamdaoui [1,2], G.S. Sahoo [3], K.G. Rodriguez-Osorio [4], M. Courel [4], M. Zazoui [5] L.M. Pérez [6], D. Laroze [7], E. Feddi [1,8]

[1]*Group of Optoelectronic of Semiconductors and Nanomaterials, ENSAM, Mohammed V University in Rabat, Morocco*
[2] *Laboratory of Condensed Matter and Interdisciplinary Sciences (LaMCScI), Faculty of Sciences Rabat, Mohammed V University in Rabat, Morocco*
[3] *School of Electronics Engineering (SENSE), Vellore Institute of Technology, Vandalur-Kellambakkam Road, Chennai, Tamil Nadu 600127, India*
[4] *Centro Universitario de los Valles, Universidad de Guadalajara, Carretera Guadalajara-Ameca, 46600, Ameca, Jalisco, Mexico*
[5] *Laboratory of Physics of Condensed Matter and Renewable Energy, Faculty of Sciences and Technology, Hassan II University of Casablanca, 146 Mohammedia, Morocco*
[6] *Departamento de Física, FACI, Universidad de Tarapacá, Casilla 7D, Arica, Chile*
[7] *Instituto de Alta Investigación, Universidad de Tarapacá, Casilla 7D, Arica, Chile*
[8] *Institute of Applied Physics, Mohammed VI Polytechnic University, Lot 660, Hay Moulay Rachid Ben Guerir, 43150, Morocco*

This study delves into the electronic and optical properties of Cu_2NiGeS_4 (CNGS) using first-principal Density Functional Theory (DFT) calculations, employing a distinctive mBJ + U potential method for precise determination of the band gap energy. CNGS, characterized by a notably high absorption coefficient (10^4 cm^{-1}), emerges as a promising candidate for photovoltaic applications. Utilizing the SCAPS-1D tool, a thin-film solar cell is simulated with a $Mo/MoS_2/Cu_2NiGeS_4$ (CNGS)/CdS/ZnO/ZnO:Al structure. The impact of factors such as layer thickness, donor and acceptor concentrations, and defect density on the CNGS layer is explored. Simulation results suggest an optimal absorption layer thickness between 2000 and 2400 nm, MoS_2 thickness of 100 nm, and a buffer layer ranging from 20 to 50 nm. Maintaining CNGS defect density below 10^{14} cm^{-3} is crucial for achieving high efficiency. Optimized outcomes reveal an efficiency conversion rate of 20.05%, a fill factor of 66.77%, a short-circuit current of 29.67 mA/cm^2, and an open-circuit voltage of 0.983 V.

[1] M. Beraich , H. Shaili, E. Benhsina, Z. Hafidi, M. Taibi, F. Bentiss, A. Guenbour ,A. Bellaouchou, A. Mzerd, A. Zarrouk, M. Fahoume. Applied Surface Science, **527**, 146800 (2020).
[2] M. Bikerouin, M. Balli, M. Farkous, M. El-Yadri, F. Dujardin, A. Ben Abdellah, E. Feddi, J.D. Correa, M.E. Mora-Ramos. Thin Solid Films, **696**, 137783 (2020).
[3] Lhoussayne Et-taya, Touria Ouslimane, Abdellah Benami. Solar Energy, **201**, 827-835 (2020).

Cation and anion ordering in synthetic lepidolites and lithian muscovites: Influence of the OH/F and Li/Al ratios on the mica formation studied by NMR spectroscopy and X-ray diffraction

Fechtelkord M.[1], Marler B.[1] and Sulcek L.[1]

[1]Ruhr-Universität Bochum, Institut für Geologie, Mineralogie und Geophysik, Bochum, Germany

A large number of lepidolites $K(Li_xAl_{3-x})[Si_{2x}Al_{4-2x}O_{10}](OH)_yF_{2-y}$ and Li-muscovites $K(Li_xAl_{2-x/3}\square_{1-2x/3})[Si_3AlO_{10}](OH)_yF_{2-y}$ were synthesised by a gelling method in combination with hydrothermal syntheses at a pressure of 2 kbar and a temperature of 873 K. The nominal composition ranged between $0.0 \leq x \leq 2.0$ and $0.0 \leq y \leq 2.0$, i.e., from polylithionite $K[Li_{2.0}Al][Si_{4.0}O_{10}](OH)_yF_{2-y}$ over trilithionite $K[Li_{1.5}Al_{1.5}][AlSi_{3.0}O_{10}](OH)_yF_{2-y}$ to muscovite $K[Al_{2.0}\square][AlSi_{3.0}O_{10}](OH)_yF_{2-y}$. ^1H, ^{19}F, ^{29}Si, ^{27}Al Magic-Angle Spinning Nuclear Magnetic resonance (MAS NMR) and ^{27}Al Multiple-Quantum Magic-Angle Spinning (MQMAS) NMR spectroscopy has been performed to investigate the order/disorder state of Si and Al in the tetrahedral layers and of Li, Al, OH and F in the octahedral layer. The synthetic mica crystals are very small, ranging from 0.1 mm to 5 mm. With increasing Al content, the crystal sizes decrease. Rietveld structure analyses showed that nearly all samples consist of two mica polytypes ($1M$ and $2M_1$) of varying proportions. In the case of lepidolites, the $1M/2M_1$-ratio depends on the Li/Al ratio of the reaction mixture. The refinement of the occupancy factors of octahedral sites shows that lepidolites ($1.5 \leq x \leq 2.0$) represent a solid solution series with polylithionite and trilithionite as the endmembers. In the case of the Li-muscovites ($0.0 \leq x \leq 1.5$) the $1M/2M_1$-ratio depends on the amount of impurity phases like eucryptite or sanidine depleting the reaction mixture of Li or Al. There is no solid solution between trilithionite and muscovite, instead, the Li-muscovite crystals consist of domains differing in the relative proportions of muscovite and trilithionite.

The overall composition of the synthesized micas which consist of two polytypes can be characterised by ^{29}Si, ^1H and ^{19}F MAS NMR spectroscopy. The Si/Al ratio in the tetrahedral layers and thus the content of $^{[4]}Al$ was calculated by analysing the signal intensities of the ^{29}Si MAS NMR experiments. The Li content x_{est} was calculated from the measured tetrahedral Si/Al ratio of the ^{29}Si MAS NMR signals. The ^{19}F and ^1H MAS NMR experiments reveal that F and OH are not distributed statistically but local structural preferences exist. F is attracted by Li-rich and OH by Al-rich environments. The ^{27}Al quadrupolar coupling constant which represents the anisotropy of the Al coordination is low for polylithionite with $C_Q = 1.5$ MHz and increases to $C_Q = 3.8$ MHz for trilithionite. For tetrahedral Al a smaller increase of C_Q from 1.7 MHz to 2.8 MHz is observed. Advancing from trilithionite to muscovite both quadrupolar coupling constants decrease to 2.5 MHz for octahedral and 1.5 MHz for tetrahedral Al. In polylithionite there is the most isotropic environment for octahedral Al, there are only Li_2Al sites coordinated by F in the octahedral sheets and O from the tetrahedral sheets which are regular containing only Si. The distortion and anisotropy for both Al in tetrahedral and octahedral sheets increases with rising Al content. The most anisotropic environment can be found in trilithionite, especially for octahedral Al [1].

^{27}Al-^{27}Al double-quantum single-quantum magic-angle spinning (DQSQ) NMR data suggests a preference for $^{[4]}Al$ in the tetrahedral sheet to occupy positions close to the $^{[6]}Al$ of the octahedral sheets [2].

[1] L. Sulcek et al. Eur. J. Miner. **35** 199-217 (2023)

[2] L. Sulcek et al. Mag. Reson. Chem. **58** 1099-1108 (2020)

Computational Investigation on Electronic Properties of Inorganic Chalcogenide Solar Absorber Material

Anima Ghosh[1, a] and R. Thangavel[2]

[1]Department of Physics, School of Sciences and Humanities, SR University, Warangal, India
[2]Department of Physics, Indian Institute of Technology (Indian School of Mines) Dhanbad, Jharkhand, India

[a]Corresponding author: animaghosh10@gmail.com

Abstract. Kesterite Cu_2ZnSnS_4(CZTS) and $Cu_2ZnSnSe_4$ (CZTSe) chalcogenide compounds are highly promising for the low-cost and high-efficient thin film solar cell technology. Herein, we have focus to show the various kesterite chalcoginide structure used for solar cell absorber materials and explore their optoelectronic properties. The electronic properties of all compounds were investigated using the highly accurate Tran–Blaha-modified Beck and Johnson (TB-mBJ) potential by the full potential linear augmented plane wave method (FP-LAPW) via Wien2K code. Electronic structure calculation predicts that these chalcogenide compounds are direct band gap semiconductors and also in good matching with the reported literature values. The total and partial density of states (DOS) of all the compounds analyzed and reported. It is further confirmed from present calculation that all the materials have high absorption coefficient values, which is suitable for solar cell. Wien2k simulation illustrated the importance and controlling of geometry to enable the progressive charge transportation of the compound.

Quantum Chemistry Topology methods for excited states. A pilot study using Benzene

Influence of Hf (0001) surface contamination on ARPES: a DFT study supporting experiments

Saleem Ayaz Khan[1], Laurent Nicolai[1], Jean Zaraket[2,3], Maria Christine Richter[2,3], Olivier Heckmann[2,3], Laxman Nagi Reddy[2,3], Waly Ndiaye[2,3], Mauro Fanciulli[2,3], Karol Hricovini[2,3], and Jan Minár[1]

[1]*New Technologies Research Centre, University of West Bohemia, CZ-30100 Pilsen, Czech Republic*
[2]*LPMS, CY Cergy Paris Université, 95031 Cergy-Pontoise, France*
[3]*Université Paris-Saclay, CEA, CNRS, LIDYL, 91191 Gif-sur-Yvette, France*

We present first ARPES studies of the electronic structure of the Hf(0001) surface. High-Z materials have attracted much interest, because the strong spin-orbit coupling in combination with the broken inversion symmetry and an important effective electric field at the surface results in a spin-momentum locking. Spin-polarized electrons at the surface are of interest in physics and novel applications in electronics and data processing. Extra sharp peaks observed in experiment are identified thanks to ab-initio calculations performed within the Wien2K and SPRKKR packages. These extra states come from oxygen contamination of the highly reactive surface of Hf(0001). Further comparison is done on the ARPES level, thanks to the one-step model which include all matrix elements effect, resulting in an excellent agreement.

A Graph Neural Network-based Algorithm for Global Optimization of Atomic Clusters

K.V. Jovan Jose

Email ID: jovanjose@uohyd.ac.in

Abstract: Exploring the evolutionary patterns and energy of metal nanoclusters to attain the lowest-energy configuration is one of the perennial problems in computational chemistry. The synergy between the electronic and geometric effects governs the stability of metal clusters [1]. However, evaluating the wavefunction and the corresponding electronic structure properties is computationally exhaustive and requires greater computational resources and time. Over the last few decades, data-driven strategies have played a significant role in understanding chemical systems [2]. In the present work, we have developed a data-driven Graph Neural Network algorithm to predict the electrostatic potential topographical (ESP) minima to assist in designing metal clusters. Further, we have exploited the directional property of ESP to obtain stable low-energy nanoclusters of varying sizes through an optimization algorithm. The benchmark studies show that this algorithm efficiently builds atomic clusters and optimizes them in minimal computational time. The oral and poster presentation details our work with benchmark studies on the Magnesium and palladium prototype nanoclusters.

1. de Heer. Walt A. The physics of simple metal clusters: experimental aspects and simple models, *Rev. Mod. Phys.* **1993**, 65,611
2. Yang, R. X.; Mc Candler, C. A.; Andriuc, O.; Siron, M.; Woods-Robinson, R.; Horton, M. K.; Persson, K. A. Big Data in a Nano World: A Review on Computational, Data-Driven Design of Nanomaterials Structures, Properties, and Synthesis. *ACS Nano* 2022, *16* (12), 19873–19891.

Computational Insights into Exciton Radiative Lifetimes in Hf-Based MXenes by many-body methods.

Nilesh Kumar,[1] Miroslav Kolos, [1] Sitangshu Bhattacharya, [2], and František Karlický [1],

1. Department of Physics, Faculty of Science, University of Ostrava, 30. dubna 22, 701 03 Ostrava, Czech Republic
2. Structure Theory Group, Department of Electronics and Communication Engineering, Indian Institute of Information Technology-Allahabad, Uttar Pradesh 211015, India

Semiconducting MXenes are an intriguing class of two-dimensional (2D) materials with promising electronic and optoelectronic properties. The presence of a band gap in semiconducting MXenes allows for efficient charge transport, making them appealing for use in a wide range of electronic device applications. Using the first-principles calculation and excited state corrections, we examined the electronic and optical properties of MXenes, $Hf_3C_2O_2$, and Hf_2CO_2 . The phonon band dispersion calculation showed the dynamically stable innovative functionalized Hf-based MXenes. We obtained the fundamental quasiparticle gap using the many-body perturbation theory. Following the Bethe-Salpeter (BSE) equation, we obtained the optical gap, binding energy, absorbance spectra, and the radiative lifetime of the exciton. Ultra-short radiative lifetimes emphasize their suitability for high-speed applications, while the significantly longer average and effective radiative lifetimes, particularly in $Hf_3C_2O_2$, underscore stability and efficiency. At room temperature, Hf 3 C 2 O 2 had an average radiative lifetime for the degenerated excitons of 11.32 & 11.42 ns and an exceptional effective radiative lifetime of 22.49 ns, indicating superior performance. In Hf_2CO_2 , a comparable trend is observed, indicating its promising potential in optoelectronic devices requiring sustained and efficient exciton behavior. These findings have important implications for the design of optoelectronic devices that require sustained and efficient exciton behavior.

Influence of defects on the structural, electronic, and optical properties of 2D-SiC and MoS$_2$

Vikram Mahamiya [1,2], Arushi Singh[2], Faiha Mujeeb[2], Subhabrata Dhar[2] and Alok Shukla [2]

[1]*The Abdus Salam International Centre for Theoretical Physics (ICTP), Strada Costiera 11, I-34151 Trieste, Italy*
[2]*Indian Institute of Technology Bombay, Powai, Mumbai 400076, India*

It is well known that the defects (dopants, vacancies, antisites, interstitials, etc.) are unavoidable during fabrication or postprocessing of materials. These defects play a crucial role in significantly tailoring the structural stability, electronic and optical characteristics of the 2D materials. Due to the quantum confinement effect of both host and defected wave functions in 2D materials, the impact of defects on the electronic and optical properties may considerably differ from their three-dimensional (3D) bulk counterparts. We have explored how various possible defects can alter the electronic and optical properties of 2D-SiC and MoS$_2$ using DFT and AIMD simulations [1,2]. Nitrogen doping is predicted to be the most favorable defect in silicon carbide monolayer due to its very low formation energy, indicating high thermodynamic stability. The analysis of the electronic band structure and the density of states shows that the additional impurity states are generated within the forbidden region in the presence of defects, leading to a significant reduction in the band gap of 2D-SiC. An interesting transition from semiconducting to metallic state is observed for N_c and Al_{Si}-defective systems. For the pristine SiC monolayer, we find that the conduction band is nearly flat in the M $\rightarrow$ K direction, leading to a high effective mass of 3.48 m_o. A significant redshift in the absorption edge, as well as the occurrence of additional absorption peaks due to the defects, have been observed in the lower energy range of the spectrum. The calculated absorption spectra span over the visible and ultraviolet regions in the presence of defects, indicating that the defective SiC monolayers can have potential optoelectronic applications in the UV-visible region. Our DFT results supports the experimental finding regarding the valley polarisation properties of MoS$_2$. The intervalley transfer process of excitons involving the Γ valley has significance in valley depolarization, especially when the layer is either under a tensile strain or has a high density of V_s defects, as these perturbations reduces K to Γ-energy separation. Band-structural calculations carried out within a density functional theory framework validate these findings.

[1]   A. Singh, V. Mahamiya, and A. Shukla, *Defect-Driven Tunable Electronic and Optical Properties of Two-Dimensional Silicon Carbide*, Phys. Rev. B **108**, 1 (2023).
[2]   F. Mujeeb, P. Chakrabarti, V. Mahamiya, A. Shukla, and S. Dhar, *Influence of Defects on the Valley Polarization Properties of Monolayer MoS2 Grown by Chemical Vapor Deposition*, Phys. Rev. B **107**, 115429 (2023).

First-principles investigations of structural and electronic properties of ternary chalcopyrite semiconductors CuInY$_2$ (Y = S, Se and Te).

Issam Mahraj [1], Andrzej Ptok [1] and Pavel Baroch [2]

[1]*Institute of Nuclear Physics, Polish Academy of Sciences,*
W. E. Radzikowskiego 152, PL-31342 Kraków, Poland
[2]*Department of Physics and NTIS – European Centre of Excellence, University of West Bohemia,*
Univerzitní 22, CZ, 306 14 Plzeň, Czech Republic

In order to investigate structural and electronic properties of CuInY$_2$ (Y = S, Se and Te), we performed first principles study within the density functional theory (DFT) as implemented in WIEN2k code [1]. The Kohn–Sham equations [2] were solved using the local density approximation (LDA) [3] and the generalized gradient approximation (GGA) in the Perdew-Burke-Ernzerhof (PBE) functional [4] for the exchange and correlation potential. The optimized lattice constants of each unit cell of our structures are obtained from minimizing the total ground energy of the structure using both LDA and GGA. To achieve more accurate electronic band structure, we employed the modified Becke-Johnson (mBJ) semilocal exchange functional [5]. Our calculation revealed that these compounds exhibit a p-type semiconductors character with a direct band gap at Γ point. The calculated band gaps energy are in good agreement with the experimental data, proves that mBJ can be an effective method for determining accurate electronic band structure of CuInY$_2$. The density of state analysis shows that these compounds are primarily influenced by the hybridization of Cu d- and Y p-states. These structures, with their suitable band gaps, are capable of absorbing a significant amount of light, thereby making them prospective choices for solar cell applications.

[1] P. Blaha, K. Schwarz, F. Tran, R. Laskowski, G.K.H. Madsen and L.D. Marks, J. Chem. Phys. **152**, 074101 (2020).
[2] W. Kohn and L. J. Sham, Phys. Rev. **140**, A1133 (1965).
[3] J. P. Perdew and Y. Wang, Phys. Rev B **45**, 13244 (1992).
[4] J. P. Perdew, K. Burke, and M. Ernzerhof, Phys. Rev. Lett. **77**, 3865 (1996).
[5] F. Tran and P. Blaha, Phys. Rev. Lett. **102**, 226401 (2009).

Table 1. Calculated and experimental crystal lattice constants a and c for $CuInY_2$ (S, Se and Te) compounds.

Crystals	a(Å)			c(Å)		
	LDA	GGA	Exp.	LDA	GGA	Exp.
$CuInS_2$	5.52	5.57	5.52	11.12	11.23	11.12
$CuInSe_2$	5.78	5.89	5.78	11.50	11.85	11.62
$CuInTe_2$	6.07	6.31	6.19	12.66	12.66	12.41

Table 2. Bulk moduli and their pressure derivatives of $CuInY_2$ compounds obtained from fit to Birch–Murnaghan equation of state.

Crystals	$B_0(GPa)$		B'_0	
	LDA	GGA	LDA	GGA
$CuInS_2$	76.57	66.70	3.14	3.76
$CuInSe_2$	62.46	57.77	2.41	3.03
$CuInTe_2$	49.85	50.16	0.72	2.25

Table 3. The calculated band gap of $CuInY_2$ (S, Se and Te) compounds in various approximations and band-gap deformation potentials.

Compounds	LDA	GGA	LDA-mBJ	GGA-mBJ	Expt.	$dE_g/dlnV$
$CuInS_2$	0.359	0.441	1.216	1.062	1.53	-3.59
$CuInSe_2$	0.264	0.206	1.001	0.713	1.04	-1.41
$CuInTe_2$	0.511	0.448	1.366	1.097	1.06	-2.89
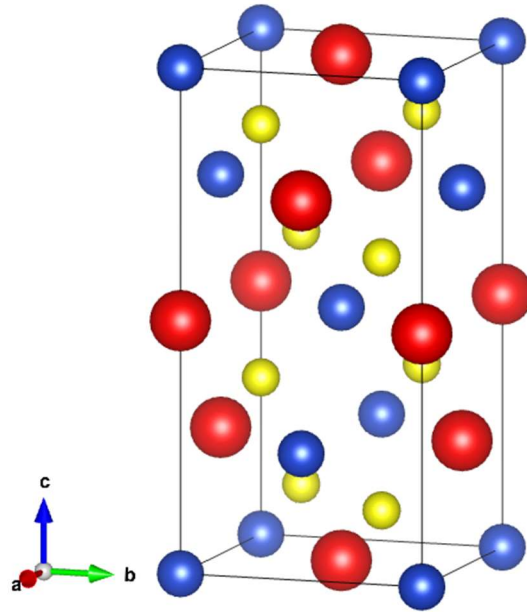
Figure. 1. The crystal structure of ternary chalcopyrite $CuInY_2$ (S, Se and Te) compounds. The Cu, In and Y ions are shown by blue, red and yellow spheres respectively.
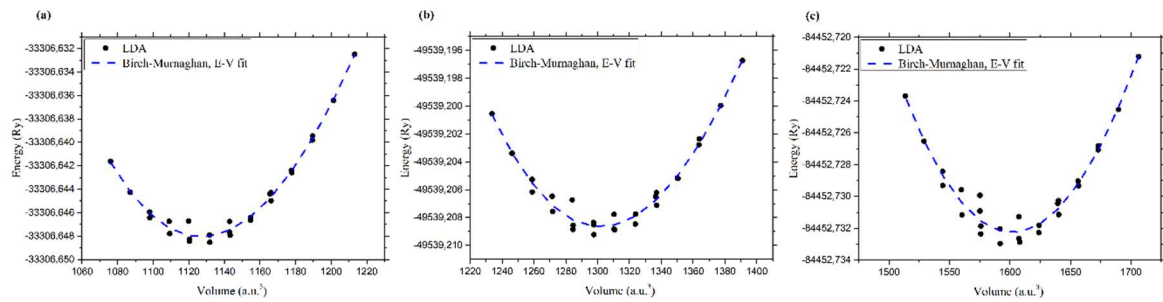

Figure. 2. The calculated total energy using LDA as function of volume: (a) $CuInS_2$. (b) $CuInSe_2$. (c) $CuInTe_2$. The fitted Birch–Murnaghan equation of state are in dashed lines.
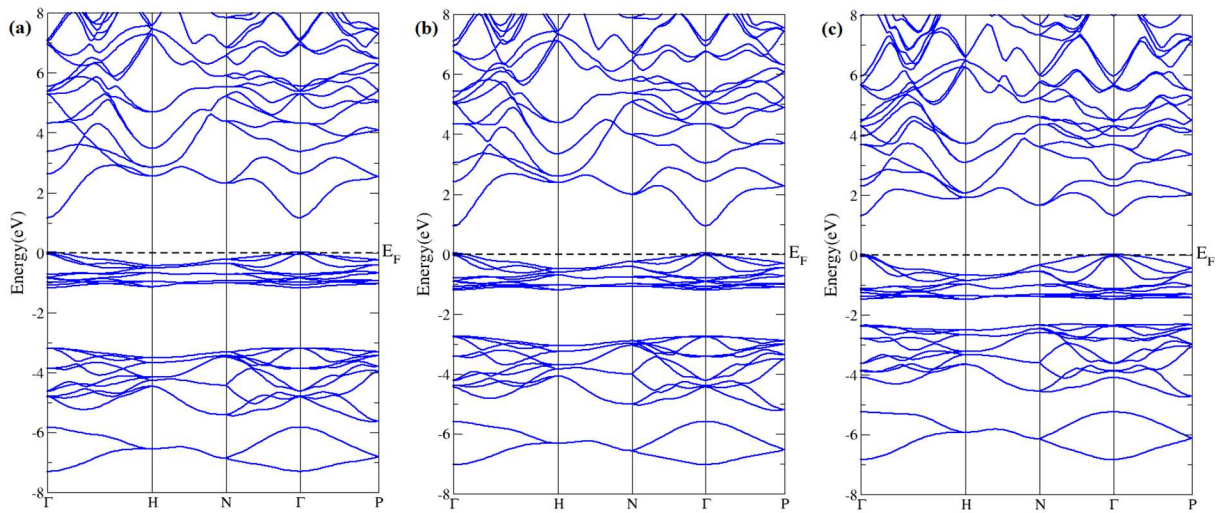

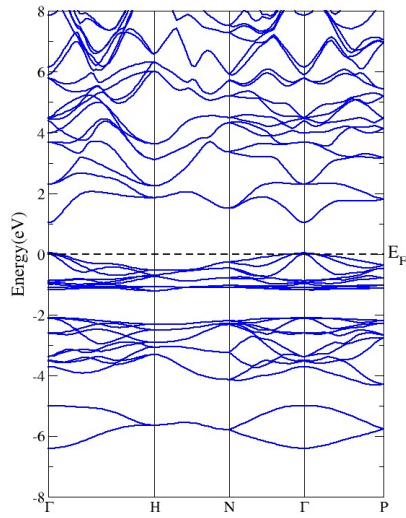**Figure. 3.** Electronic band structure of $CuInY_2$ compounds using LDA-mBJ: (a) $CuInS_2$, (b) $CuInSe_2$, (c) $CuInTe_2$.

Figure. 4. Electronic band structure of $CuInTe_2$ compound using GGA-mBJ.
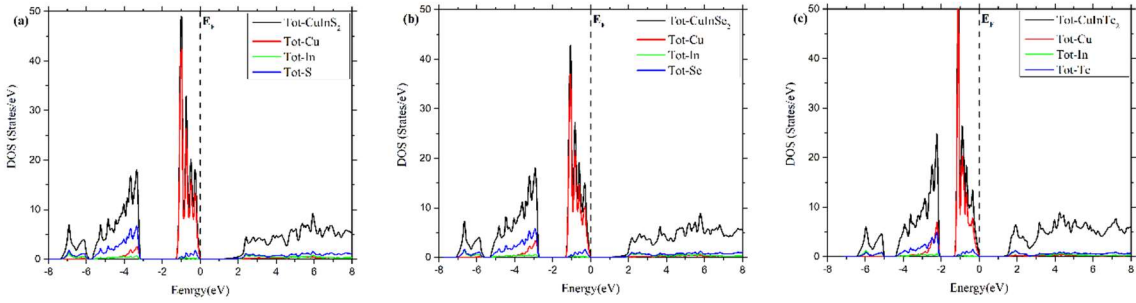
Figure. 5. Total density of states of $CuInY_2$ compounds: (a) $CuInS_2$, (b) $CuInSe_2$, (c) $CuInTe_2$.
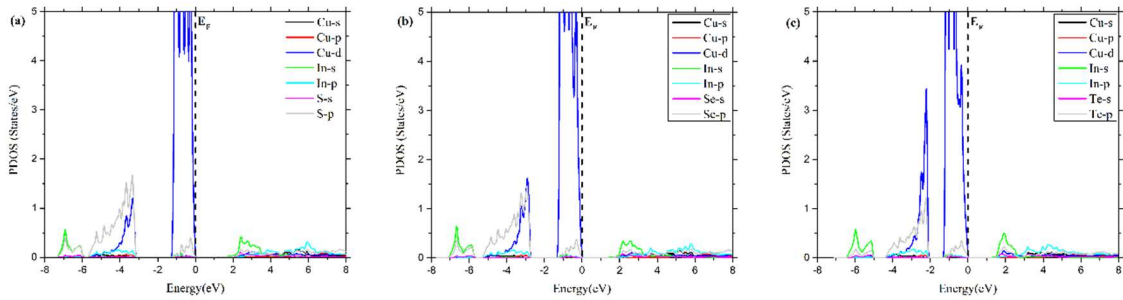

Figure. 6. Partial density of states of $CuInY_2$ compounds: (a) $CuInS_2$, (b) $CuInSe_2$, (c) $CuInTe_2$.

Tight-binding model for the electronic structure of Lu2CF2 2D MXene based on the WIEN2k calculation

Alireza Mostafaei[1] and Ebrahim Heidari Semiromi[1]

[1]Department of Physics, University of Kashan, Kashan, 87317-53153, Iran.

The family of two-dimensional transition metal carbides and nitrides, known as MXenes, has attracted substantial attention in science and technology. We obtain a parameterized minimal tight-binding model to provide an accurate description of both valence and conduction bands of Lu_2CF_2 MXene based on the band structures obtained within the framework of density functional theory by WIEN2k. It is shown that the next nearest-neighbor 13-band p3d5 model is fairly sufficient to describe the electronic structure of these systems over a wide energy range. The obtained hopping and Slater–Koster parameters can be used to study the physical properties of MXene based materials and nanostructures in the framework of the tight-binding model.

P22

Investigation of local dielectric function of HfO$_2$ thin layers with different crystallographic phases by EELS Analysis and DFT Simulations

Vargas, Beatriz [1]; Nandi, Pranjal [1]; Nasiou, Déspina [2]; Molina-Luna, Leopoldo [2]; Coll, Catalina[3], del Pozo Bueno, Daniel [1]; Kaiser, Nico [4]; Schreyer, Philipp [4]; Alff, Lambert [4]; López-Conesa, Lluís[1,5]; Peiró, Francesca[1] ; Yedra, Lluís [1, 6]; Estradé, Sonia [1]

[1] LENS-MIND, Department of Electronics and Biomedical Engineering and Institute of Nanoscience and Nanotechnology (IN2UB), University of Barcelona (UB), Barcelona, Spain.

[2] Advanced Electron Microscopy Division,Institute of Materials Science, TU Darmstadt, 64287, Darmstadt, Germany.

[3] Catalan Institute of Nanoscience and Nanotechnology (ICN2), CSIC and BIST, Campus UAB, Bellaterra, Spain.

[4] Advanced Thin–Advanced Thin Film Technology Division,Institute of Materials Science, TU Darmstadt, 64287, Darmstadt, Germany.

[5] Scientific and Technological Centers of the Universitat de Barcelona (CCiTUB).

[6] Department of Physics, Universitat Politècnica de Catalunya · BarcelonaTech, Barcelona, Spain.

Hafnium oxide (HfO$_2$) is a material with a high dielectric response, making it widely used in the fabrication of advanced semiconductor devices. The dielectric function is an important parameter in the study of its optical and electronic properties [1]. At the nanoscale, the dielectric response of HfO$_2$ can differ from its behavior in bulk, due to a variety of factors such as defects and surface effects [2].

In this study, we compare the dielectric function and energy loss function of HfO$_2$ thin layers using experimental as well as DFT simulations, for the monoclinic and rhombohedral phases. Thin films of 20 nm HfO$_{2-x}$ were grown on a c-cut sapphire substrate. The hafnium layers were grown from metallic hafnium and a controlled flux of oxygen radicals at an RF plasma power of 200 W and a substrate temperature of 320 °C. The monoclinic hafnium oxide was grown at a hafnium rate of 0.1 A/s with an oxygen flux of 0.18 sccm. The rhombohedral hafnium oxide was grown at a hafnium rate of 0.9 A/s at an oxygen flow of 0.1 sccm. The TiN was grown at a substrate temperature of 800 °C from a Ti source with an evaporation rate of 0.2 A/s and an RF plasma power of 340 W. Subsequently, a Pt electrode was deposited in vacuum using molecular beam epitaxy (MBE), obtaining two multilayer devices as shown in Fig. 1 [3,4]. Electron transparent cross-sectional TEM lamellas were fabricated using a JEOL 4600F Focused Ion Beam (FIB), and EELS data were acquired in a JEOL-ARM200F at 200 kV.

The dielectric function and electron energy loss function of HfO$_2$ have been extracted from electron energy loss spectra (EELS) by Kramers-Kronig (KK) analysis, using the algorithm reported by Eljarrat [5]. The effects of crystalline structure on the optical properties of HfO$_2$ have been observed through the analysis of the dielectric function, both, experimentally as well as theoretically as shown in Fig. 2. Additionally, for each sample, the procedure was applied to two different layers in the hafnium layer with different concentration of oxygen in order to observe how the oxygen variation affects the optical response. KK calculations, upon comparison, reveals that the oxygen rich rhombohedral phase transforms into a monoclinic phase. Further, Density Functional Theory (DFT) calculations also support the experimental findings.
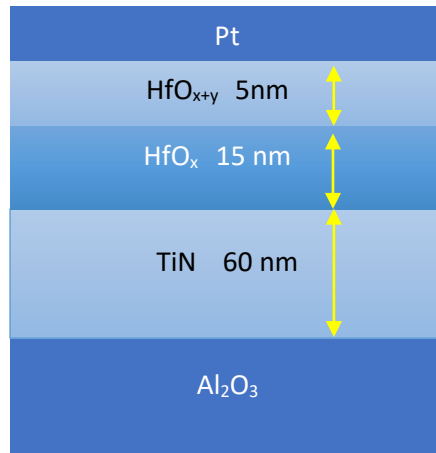
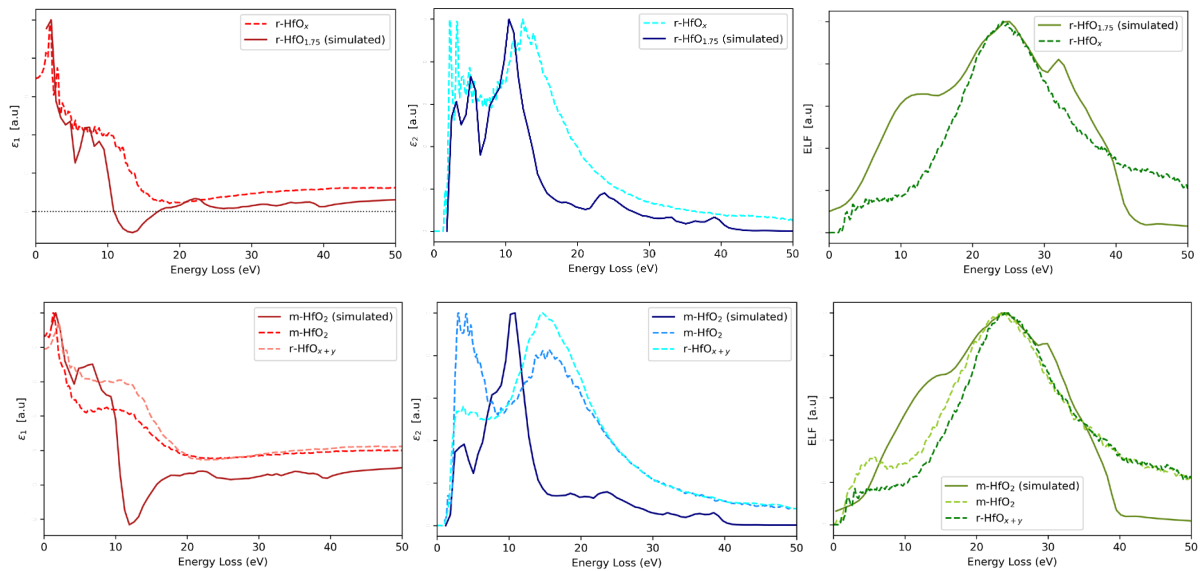Figure 1: Image depicting the layers in the sample (figure not to scale)

Figure 2: Comparison of both dielectric and ELF response between DFT simulations and experimental data of monoclinic and rhombohedral phases.

Acknowledgements

References

[1] E. I. Suvorova, O. V. Uvarov, N. A. Arkharova, A. D. Ibrayeva, V. A. Skuratov, and P. A. Buffat. Structure evolution, bandgap, and dielectric function in La-doped hafnium oxide thin layer subjected to swift Xe ion irradiation. *J Appl Phys*, vol. 128, no. 16, Oct. 2020, doi: 10.1063/5.0025536.

[2]   J. Park and M. Yang, 'Determination of complex dielectric functions at HfO2/Si interface by using STEM-VEELS', *Micron*, vol. 40, no. 3, pp. 365–369, Apr. 2009, doi: 10.1016/J.MICRON.2008.10.006.

[3]   Nico Kaiser, Tobias Vogel, Alexander Zintler, Stefan Petzold, Alexey Arzumanov, Eszter Piros, Robert Eilhardt, Leopoldo Molina-Luna, and Lambert Alff, Defect-Stabilized Substoichiometric Polymorphs of Hafnium Oxide with Semiconducting Properties, ACS Applied Materials & Interfaces 2022 14 (1), 1290-1303, DOI: 10.1021/acsami.1c09451

[4]   Nico Kaiser, Young-Joon Song, Tobias Vogel, Eszter Piros, Taewook Kim, Philipp Schreyer, Stefan Petzold, Roser Valentí, and Lambert Alff, Crystal and Electronic Structure of Oxygen Vacancy Stabilized Rhombohedral Hafnium Oxide, ACS Applied Electronic Materials 2023 5 (2), 754-763, DOI: 10.1021/acsaelm.2c01255

[5]   A. Eljarrat and C. T. Koch. Design and application of a relativistic Kramers–Kronig analysis algorithm. *Ultramicroscopy*, vol. 206, Nov. 2019, doi: 10.1016/j.ultramic.2019.112825.

An investigation of the W-Ta-Vacancy system: A combined DFT and Cluster expansion study

Dhanshree Pandey[1], Nicola Seriani[1], Ralph Gebauer[1], Christian Hill[2], Kalle Heinola[2]

[1]*The Abdus Salam International Centre for Theoretical Physics, Strada Costiera 11, 34151, Trieste, Italy*
[2]*International Atomic Energy Agency, Vienna International Centre, P.O. Box 100, A-1400 Vienna, Austria*

Tungsten (W) is a notable choice for plasma-facing materials (PFM) due to its high melting point and minimal erosion rates. However, its advantage is counterbalanced by a significant drawback: a notable lack of fracture toughness leading to brittle failure patterns. To address these challenges, we explore the incorporation of alloying elements[1]. In alloys, the formation energy depends on the spatial arrangement of diverse atoms around vacant sites, making the vacancy concentration a function of the alloy composition. In this study, we treat mono-vacancies as an additional 'chemical' component in W-based alloys. Consequently, we calculate the phase diagram of W-Ta-Vacancy (WTaVac) by combining first-principles energy methods and Monte Carlo simulations.

Over 400 structures representing different ordered arrangements of W/Ta and mono-vacancies within the bcc W host undergo first-principles total-energy calculations. These energies then parameterize a cluster expansion describing the energy of the WTaVac system using an Ising-like Hamiltonian. Identifying stable structures at low temperatures involves constructing the convex hull of formation energies. A well-converged cluster expansion with approximately 8 meV/atom cross-validation is employed in Monte Carlo (MC) simulations to determine thermodynamic properties. The MC simulation outcomes reveal vacancy clustering, with Ta atoms predominantly surrounding the vacancy clusters.

This preference of Ta atoms surrounding the vacancy is further supported by DFT calculations when creating a mono-vacancy in W-Ta alloy of different sizes.

In conclusion, these results suggest that vacancies induce partial segregation in the alloys, which could influence their mechanical properties.

[1] O. El-Atwani et al., Sci. Adv., **5**, eaav2002 (2019).

Abstract template for … PY-Nodes: An ab-initio python code for searching nodes in a material using Nelder-Mead's simplex approach…

Vivek Pandey [1] and **Sudhir K. Pandey** [2]

[1] *School of Physical Sciences, Indian Institute of Technology Mandi, Kamand 175075, India*
[2] *School of Mechanical and Materials Engineering, Indian Institute of Technology Mandi, Kamand 175075, India*

With the discovery of topological semimetals, it has been found that the band touching points near the Fermi level are of great importance. They give rise to many exciting phenomena in these materials. Moreover, these points, commonly known as nodes, are related to several properties of these semimetals. Thus, the proper estimation of their coordinates is extremely needed for better understanding of the properties of these materials. We have designed a Python 3 based code named *PY-Nodes* for efficiently finding the nodes present in a given material using *first-principle* approach [1]. The present version of the code is interfaced with the WIEN2k package. For benchmarking the code, it has been tested on some famous materials that possess characteristic nodes. These include– TaAs, a well-known Weyl semimetal [2], Na_3Bi, which is categorized as Dirac semimetal [3], CaAgAs, classified as a nodal-line semimetal [4] and YAuPb, which is claimed to be non-trivial topological semimetal [5]. In the case of TaAs, 24 nodes are obtained from our calculations. On computing their chiralities, it is found that 12 pairs of nodes having equal and opposite chirality are obtained. Furthermore, for Na_3Bi, a pair of nodes are obtained on either side of the Γ-point in the k_3 direction. In the case of CaAgAs, several nodes are obtained in the k_z=0 plane. These nodes, when plotted in the k_x-k_y plane, form a closed loop which is generally referred to as a nodal-line. Finally, in the case of YAuPb, large number of nodes are obtained in the vicinity of Γ-point. The results obtained for these materials are in good match with the previous works carried out by different research groups. This assures the reliability and efficiency of the *PY-Nodes* code for estimating the nodes present in a given material.

[1] V. Pandey, S. K. Pandey, Comput. Phys. Commun. **283**, 108570 (2023).
[2] S.-Y. Xu, I. Belopolski, N. Alidoust, M. Neupane, G. Bian, C. Zhang, R. Sankar, G. Chang, Z. Yuan, C.-C. Lee, S.-M. Huang, H. Zheng, J. Ma, D.S. Sanchez, B. Wang, A. Bansil, F. Chou, P.P. Shibayev, H. Lin, S. Jia, M.Z. Hasan, Science. **349**, 613617 (2015).
[3] G.S. Jenkins, C. Lane, B. Barbiellini, A.B. Sushkov, R.L. Carey, F. Liu, J.W. Krizan, S.K. Kushwaha, Q. Gibson, T.R. Chang, H.T. Jeng, H. Lin, R.J. Cava, A. Bansil, H.D. Drew, Phys. Rev. B **94,** 085121 (2016).
[4] X.B. Wang, X.M. Ma, E. Emmanouilidou, B. Shen, C.H. Hsu, C.S. Zhou, Y. Zuo, R.R. Song, S.Y. Xu, G. Wang, L. Huang, N. Ni, C. Liu, Phys. Rev. B. **96,** 161112 (2017).
[5] F. Tang, H.C. Po, A. Vishwanath, X. Wan, Nature **566**, 486489 (2019).

Topological Insulating Phase in Non-centrosymmetric LiSrBi Compound

Saurav Patel [1] , Paras Patel [1,2] , Bhautik R. Dhori [1,2] , and Prafulla K. Jha [2]

[1]Department of Physics, Faculty of Science, The Maharaja Sayajirao University of Baroda, Vadodara, Gujarat, India-390002.

In the realm of condensed matter physics, investigation of nontrivial band topology holds immense potential for exploring intercorrelation between topology and symmetry [1]. Particularly, topological insulators (TIs) gained surge research interest owing to their intriguing properties, such as gapless boundary states, unconventional spin texture and so on. These materials hold great promise for diverse applications, including spintronics, quantum computing and thermoelectric devices. The TI properties can be realised by bulk band inversion mechanism owing to spin-orbit coupling (SOC). The Non-centrosymmetric materials offer a diverse range of topologically intriguing compounds [2]. By leveraging the tunability of their hybridization strength through lattice parameters, we investigate the potential of achieving a topological insulating phase in the novel LiSrBi compound using the first-principles calculation within the framework of density functional theory. All calculations were performed in the Vienna Ab Initio Simulation Package. The dynamical, mechanical and thermal stability is confirmed from phonon dispersion curves, elastic constants and molecular dynamics. The LiSrBi compound exhibits direct band gap of 0.10 eV with SOC. We have applied biaxial strain along [110] direction and hydrostatic pressure to enginner the band topology in LiSrBi. This leads to the $-s$ and $-p_z$ orbital inversion of Sr and Bi, respectively at the Γ point ensuring the trivial to non-trivial topological phase transition (TPT). The TPT occurs at ~1.7% (~1.4%) for biaxial strain (hydrostatic pressure) and retain its nontrivial band ordering even at higher strain (hydrostatic pressure). Tight-binding Hamiltonian are constructed using WANNIER90 package based on the maximally localized Wannier functions which is used in WANNIERTOOLS to obtain the surface states and Z_2 invariants. Our results indicate that LiSrBi shows topological insulating characteristics and can have promising implications for applications in nano-electronics and spintronics.

[1] Hasan M. Zahid, Charles L. Kane, Rev. Mod. Phys. **82**, 3045 (2010).
[2] C. Mondal, C Barman, S. Kumar, A. Alam, B. Pathak, Scientific reports **9**, 527 (2019).

Computational modelling of all-solid state batteries containing Li_2S-P_2S_5 glasses as an electrolyte.

J. Pawelko[1,2], X. Rocquefelte[1], E. Furet[2]

[1] Université de Rennes CNRS, ISCR (Institut des Sciences Chimiques de Rennes) - UMR 6226, F-35000 Rennes, France

[2] École Nationale Supérieure de Chimie de Rennes CNRS, ISCR (Institut des Sciences Chimiques de Rennes) - UMR 6226, F-35000 Rennes, France

Rechargeable batteries that contain anodes made of lithium are interesting due to their high capacity and low electrochemical potential. The most common lithium batteries right now are made with liquid electrolytes which results in problems connected to poor cycle performance and safety hazards due to dendrite growth[1, 2]. Solution to this problems may be switching to solid electrolytes like glasses which are also characterised by high conductivity.

Compositions based on Li_2S-P_2S_5 are well-known ionic conductors, making them good candidates as solid state electrolytes [3, 4]. Previous research efforts performed on this ternary system proves that the ionic conductivity of the amorphous structure 75mol% Li_2S – 25mol% P_2S_5 is the highest because it possesses the balance between density and diffusibility of Li^+ [5].

The aim of the present work is to investigate the relation between the composition of the glass and its conductivity by means of Born-Oppenheimer Molecular Dynamics simulations in order to characterise the atomic scale structure of the experimental compositions. In addition, we will analyse the impact of intrinsic and extrinsic defects on the properties of the related crystalline phases.

[1] D. P. Lv, Y. Y. Shao, T. Lozano, W. D. Bennett, G. L. Graff, B. Polzin, J. G. Zhang, M. H. Engelhard, N. T. Saenz, W. A. Henderson, P. Bhattacharya, J. Liu, J. Xiao, Adv. Energy Mater., **5,** 1402290 (2015).

[2] W. Xu, J. L. Wang, F. Ding, X. L. Chen, E. Nasybutin, Y. H. Zhang, J. G. Zhang, Energy Environ. Sci., **7**, 513–537 (2014).

[3] F. Mizuno, A. Hayashi, K. Tadanaga, M. Tatsumisago, Adv. Mater. **17,** 918–921 (2005).

[4] A. Hayashi, S. Hama, H. Morimoto, M. Tatsumisago, T. Minami, J. Am. Ceram. Soc. **84,** 477–479 (2001).

[5] T. Baba, Y. Kawamura Front. Energy Res. **4**, 22 (2016).

Nonzero spontaneous electric polarization in metals: Novel predictive methods and applications

Shahrbano Rahimi-[1], S. Jalali-Asadabadi [1], Peter Blaha[2], and Farhad Jalali-Asadabadi [1]

[1]*Department of Physics, Faculty of Physics, University of Isfahan (UI), Hezar Jerib Avenue, Isfahan 81746-73441, Iran*
[2] *Institute of Materials Chemistry, Vienna University of Technology, Getreidemarkt 9/165-TC, A-1060 Vienna, Austria*

Ferroelectricity in metals has advanced since the initial discovery of nonmagnetic ferroelectric-like metal $LiOsO_3$ [1], anchored in the Anderson and Blount prediction [2]. However, evaluating the spontaneous electric polarization (SEP) of this metal has been hindered by experimental and theoretical obstacles [3,4]. The experimental challenge arises from difficulties in switching polarization using an external electric field, while the theoretical limitation lies in existing methods applicable only to nonmetals. Zabalo and Stengel [5] addressed the experimental obstacle by proposing flexoelectricity as an alternative for practical polarization switching in $LiOsO_3$, which requires a critical bending radius similar to $BaTiO_3$. In this study, we focus on resolving the theoretical obstacle by modifying the Berry phase and Wannier functions approaches within density functional theory plus modern theory of polarization. By employing these modifications, we calculate the SEP of $LiOsO_3$, comparable to the polarization of $BaTiO_3$. We validate our predictions using various ways. This study confirms the coexistence of ferroelectricity and metallicity in this new class of ferroelectric-like metals. Moreover, by addressing the theoretical limitation and providing new insights into polarization properties, our study complements the experimental flexoelectricity proposal and opens avenues for further exploration and manipulation of polarization characteristics. The developed approaches, incorporating modified Berry phase and Wannier function techniques, offer promising opportunities for studying and designing novel materials, including bio- and nano-ferroelectric-like metals. This study contributes to the advancement of ferroelectricity in metals and provides a foundation for future research in this exciting field.

[1] Shi, Y. et al. Nat. Mater. **12**, 1024 (2013).
[2] Anderson, P. W. & Blount, E. Phys.Rev. Lett. **14**, 217 (1965).
[3] Jinlian, Lu. et al. Phys. Rev. Lett. **122**, 227601 (2019).
[4] Rui-Chun Xiao. et al. PRB 102, 024109 (2020).
[5] Zabalo, A. & Stengel, M. Phy. Rev. Lett. **126**, 127601 (2021).

The structure and properties of bilayer borophene

Subrata Rakshit and Nevill Gonzalez Szwacki

Institute of Experimental Physics, Faculty of Physics, University of Warsaw, Pasteura 5, PL-02093 Warsaw, Poland

Borophene is a crystalline atomic monolayer of boron that exhibits several polymorphic forms [1]. In recent years, borophene has been identified as a rising star in materials science for the development of sensors, energy storage devices, and batteries.

Very recently it was experimentally demonstrated [2] the synthesis of an atomically well-defined borophene polymorph beyond the single-atomic-layer limit. The structure of the bilayer borophene is consistent with two covalently bonded α-sheets. While these sheets retained the highly desirable electrical and mechanical properties of single-layer borophene, it is proposed that the space between the layers could be used for energy or chemical storage. For example, the inclusion of a layer of lithium ions could enable the manufacture of 2D batteries.

In this work, we present the results of first-principles calculations for double-layer boron structures consisting of hexagonal, α-sheet, or honeycomb boron layers (see Fig. 1). Different arrangements between the layers have been considered. For the most stable structures, the electronic, elastic, and transport properties are studied. According to our calculations, the high metallic character of borophenes is, in most cases, preserved also for the double-layer structures. Also, the structural stability of the single layers is reinforced by the presence of interlayer bonds.
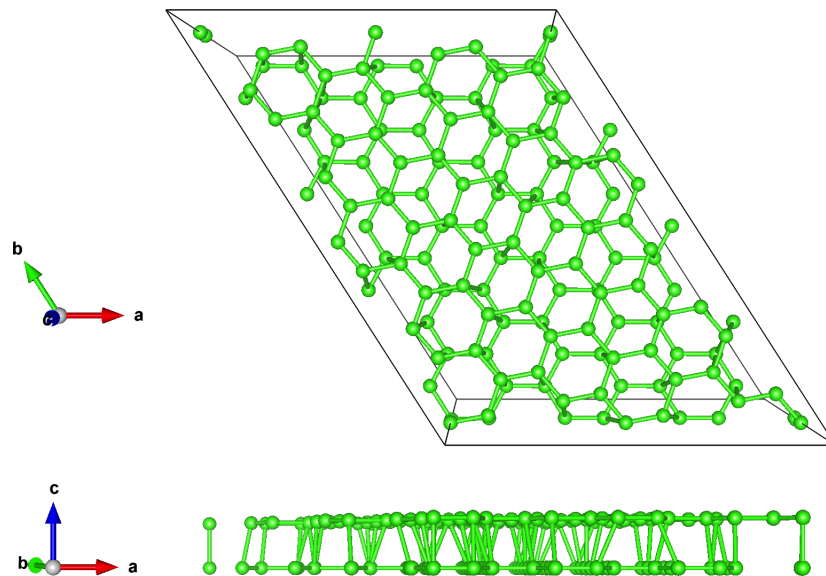

Figure 1: The atomic structure of double layer borophene. The single layers are boron honeycomb (hc) structures. The bottom panel shows the bonding between the layers.

[1] T. Tarkowski, N. Gonzalez Szwacki, and M. Marchwiany, *Phys. Rev. B* **104**, 195423 (2021).

[2] X. Liu et al., *Nat. Mater.* **21**, 35 (2022).

Dopants effect on the electronic and catalysis properties of Silver oxides: DFT

Habib Rozale [1], A. AMAR[1], and A. CHAHED[1]

[1]([1]Condensed Matter and sustainable development Laboratory (LMCDD), University of Sidi Bel-Abbes, Sidi Bel-Abbes 22000, Algeria

We study, by first-principles calculations, the structural, electronic and stability of Ag_2O and Ag_2S compounds in the cuprite structure, a detailed understanding of the electronic properties of silver-(oxygen and sulfur based) compounds would be valuable. The FP-LAPW method within the GGA-PBE, TB-mBJ and HSE06 functional approximations is chosen in the computational approach. The computed lattice constant for Ag_2O and Ag_2S was found to agree with the available theoretical and experimental results. For electronic properties the reproduction of the experimental band gap energy is seen with the hybrid-DFT functional HSE06, compared to GGA-PBE and for TB-mBJ. In order to better understand the behavior of electronic states of Silver-based compounds, a detailed of the electronic properties would be valuable. It is believed that the change of the Fermi level of a semiconductor will definitely affect its photocatalytic properties due to the contribution of both strong hybridization between the O and S p states and Ag d states. From the optical results we show that the studied materials are important for optoelectronics device because he exhibited wide range of absorption spectra.

Thermoelectric Performance of Li-based Half-Heusler Alloys: A First-Principles Investigation

Sangeeta [1], and Mukhtiyar Singh [1]

[1] *Department of Applied Physics, Delhi Technological University,*
Delhi-110042, India

Li-based 8-valence electron half Hesuler alloys can be promising thermoelectric materials owing to their intriguing properties such as high mechanical strength, dynamically stable, and good transport properties [1]. Thus, in this study we systematically investigate the structural, dynamical, thermal, and transport properties of LiCaAs and LiCaSb half Heusler alloys using first-principles calculations. The dynamical and thermal stability of these alloys are confirmed using phonon dispersion calculations and ab-initio molecular dynamic simulations. The Tran-Blaha modified Becke Johnson functional [2] was employed for electronic structure calculations to determine the band gap and transport properties of investigated alloys. The Boltzmann Transport equation was solved to derive the transport properties for both p-type and n-type doping over a temperature range of 300 K to 800 K [3]. The relaxation time of these studied compounds at varying temperatures is computed through the utilisation of deformation potential theory [4]. At an optimised carrier concentration, the p-type LiCaAs exhibits a large power factor of 10.95×10^{11} $Wm^{-1}K^{-2}s^{-1}$, while LiCaSb have value of 12.53×10^{11} $Wm^{-1}K^{-2}s^{-1}$. The low lattice thermal conductivities are obtained for both alloys. At 800 K, the p-type of LiCaAs compound exhibits ZT of ~ 0.90 and LiCaSb exhibits ZT of ~ 0.93 at carrier concentration of $\sim 10^{20}$ cm^{-3}. The thermoelectric performance exhibited by investigated alloys indicating they hold potential as suitable candidates for energy harvesting applications.

[1] J-L. Xiong, F. Yu, J. Liu, X-C. Liu, Q. Liu, K. Liu, S-Q Xia, ACS Appl. Energy Mater. **5,** 3793-3799 (2022).
[2] F. Tran, P. Blaha, Phys. Rev. Lett. **102,** 5–8 (2009).
[3] G.K. Madsen, D.J. Singh, Comput. Phys. Commun. **175**, 67–71 (2006).
[4] J. Bardeen, W. Shockley, Phys. Rev. **80**, 72-80 (1950).

Novel two-dimensional room-temperature ferromagnetic rare-earth material - GdB2N2 with large perpendicular magnetic anisotropy

G.C. Shan [1] , **H.Y. Tan** [1,2] , and **J.L. Zhang** [2]

[1]*Beihang University, Beijing, China*
[2] *Institute of Advanced Studies, City University of Hong Kong, Hong Kong SAR*

Two-dimensional (2D) ferromagnets with large magnetic anisotropy are promising in modern spintronics, but low Curie temperature and small magnetic anisotropy energy (MAE) hinder their applications seriously. Herein, by employing density functional theory (DFT) calculations, we predict a new kind of 2D ferromagnetic materials - GdB2N2, which possesses large magnetic moment ($\sim$7.87 µB/f. u.), very high Curie temperature ($\sim$335 K) and large perpendicular magnetic anisotropy ($\sim$10.38 meV/f. u.). Biaxial strain ranging from -0.5% to 5% and different concentrations of charge-carrier doping ($\leqslant$0.5 e/h per f. u.) are further applied to reveal the influence on the Curie temperature and MAE. The magnetic ordering of GdB2N2 is found dominated by a Ruderman-Kittel-Kasuya-Yosida (RKKY) mechanism. The prediction of such a novel 2D ferromagnet presented here, not only enriches the family of 2D ferromagnetic materials, but also makes it possible to combine traditional 2D materials and rare-earth metals for achieving more intriguing magnetic properties, which could eventually carve out a new path for the next-generation spintronic devices and sensors.

[1] H. Tan, G.C. Shan, and J.L. Zhang, Prediction of room temperature ferromagnetism 2D GdB2N2 with large perpendicular magnetic anisotropy, Materials Today: Physics **24**,100700 (2022).
[2] H. Tan, G.C. Shan, and G. Pacchioni, Prediction of 2D ferromagnetism and monovalent europium ions in the EuBr/graphene heterojunctions, Phys. Chem. Chem. Phys., **23**, 25500-25506 (2021).

Ab-initio Study on CsNdNb$_2$O$_7$ and CsLaNb$_2$O$_7$ Dion-Jacobson Perovskites

Pedro A. Sousa[2], **Helena M. Petrilli**[1], **António N. Cesário**[1], **Lucy Assali**[2], **E. Lora da Silva**[1], **P. N. Lekshmi**[1], **P. Rocha Rodrigues**[1], **S.S.M.Santos**[3], **J. G. Correia**[4], **J. P. Araújo**[1] and **A. M. L. Lopes**[1]

[1]*(Presenting author underlined) IFIMUP, Faculdade de Ciências da Universidade do Porto, Portugal*
[2]*Instituto de Fisica da Universidade de São Paulo, São Paulo, Brazil*
[3]*Escola Politécnica da Universidade de São Paulo, São Paulo, Brazil*
[4]*C2TN, Centro de Ciências e Tecnologias Nucleares, Departamento de Engenharia e Ciências Nucleares, Instituto Superior Técnico, Portugal*

According to Benedek et. al [1], the CsNdNb$_2$O$_7$ system undergoes two phase transitions, one at 625 K and another at 800 K. Our objective is to investigate those three distinct phases: $P2_1am$ (# 26), $C2/m$ (# 12) and $P4/mmm$ (# 123) [1]. There is no existing literature discussing the magnetic state of CsNdNb$_2$O$_7$. Nevertheless, due to the presence of three unpaired electrons in the $4f$ orbital of the Nd atoms, this material is expected to exhibit magnetic properties. Benedek and her research group simulated the system by freezing the $4f^3$ electrons in the core [2], employing a non-polarized simulation. We initiated our study with an investigation into the optimal approach for simulating the CsNdNb$_2$O$_7$ system. To accomplish this, we conducted a thorough analysis by comparing spin-polarized with Hubbard correction and non-polarized models. We demonstrated the necessity of a Hubbard correction for the spin-polarized model, wherein we obtained an *ab-initio* estimate of the Hubbard parameter as 4.15 eV for the $P4/mmm$ (aristotype) phase. This value is in our spin-polarized simulations, although further investigation is being held to obtain an accurate estimate for the ground state. Additionally, we expanded our investigation to include the CsLaNb$_2$O$_7$ system, which exhibits non-magnetic characteristics, thereby offering a valuable point of comparison in our study. Thus, through the analysis of the Density of States (DOS) and the Electrical Field Gradients (EFG) of the different models, we will determine the optimal approach for simulating CsNdNb$_2$O$_7$ and potentially other members of the Dion-Jacobson family of naturally layered perovskites.

[1] Zhu T., Gibbs A.S., Benedek N.A. and Hayward M.A., Chemistry of Materials 32, 10, 4340–4346 (2020).
[2] Benedek N.A., Inorganic Chemistry 53, 7, 3769–3777 (2014).

AMCHECK: a tool to check whether a symmetry-compensated collinear magnetic material is antiferro- or altermagnetic

Andriy Smolyanyuk[1]**, Libor Šmejkal**[2]**, and Igor I. Mazin**[3]

[1] *Institute of Solid State Physics, TU Wien, 1040 Vienna, Austria*
[2] *Johannes Gutenberg Universität Mainz, Mainz, Germany*
[3] *George Mason University, Fairfax, USA*

Up to now only a limited amount of altermagnetic materials were reported and a tool to predict if a given material is an altermagnet or not would be of great use for seeking new altermagnetic candidates. Utilizing the fact that the magnetic moment compensation in these systems is driven by symmetry, we developed a program/library that allows one to check if the given material is an altermagnet by using information about its crystal structure and magnetic pattern.

Magnetism and magnetic anisotropy of a single rare-earth atom on transition metal dichalcogenides: A first-principles prediction

T. Ochirkhuyag [1,2], **N. Batnyam** [1,2], **B. Odontuya** [1], **M. Gonchigsuren** [1], **and D. Odkhuu** [1,2,3]

[1] *School of Applied Sciences, Mongolian University of Science and Technology, Ulaanbaatar 14191, Mongolia*
[2] *Department of Physics, Incheon National University, Incheon 22012, South Korea*
[3] *Institute of Physics and Technology, Mongolian Academy of Sciences, Ulaanbaatar 13330, Mongolia*

Exploring magnetism in otherwise nonmagnetic two-dimensional materials, such as graphene and transition metal dichalcogenides (TMDs), is at the heart of spintronics research. Employing systematic density-functional theory [1,2] and Monte Carlo simulations [3,4], we have studied the energetics and magnetism of a series of rare-earth (RE) atoms on WSe_2 and MoSe2 monolayers with various possible natural defects. In this talk, we will emphasize on significantly large perpendicular magnetocrystalline anisotropy (PMA) up to an order of 10 meV predicted in WSe_2 with Nd and Sm substitutions for the W site. Numerical results of PMA are elucidated in terms of an energy level change in the large spin-orbit coupled RE $4f$ – W $5d$ orbital states that are hybridized with the Se $4p$ orbital states in the low-spin bipyramidal crystal field. The present argument is also applicable for $MoSe_2$. The RE concentration and strain dependences of magnetic moment and PMA, and its underlying mechanism will also be discussed.

[1] P. Blaha, K. Schwarz, G. K. H. Madsen, D. Kvasnicka, and J. Luitz, (Technische Universitat Wien, 2001).
[2] G. Kresse and J. Hafner, Phys. Rev. B **47**, 558(R) (1993).
[3] P. Asselin, Phys. Rev. B **82**, 054415 (2010).
[4] N. Metropolis, A. W. Rosenbluth, M. N. Rosenbluth, A. H. Teller, and E. Teller, J. Chem. Phys. **21**, 1087 (1953).

Interaction mechanism of rare earths with γ-Graphyne: Comparative analysis using an all-electron and pseudoelectron-based DFT approach

Antara Vaidyanathan [1], Avinash Pardhi [1], Vaibhav Wagh[1], and Brahmananda Chakraborty [2,3]

[1]*Department of Chemistry, Ramnarain Ruia Autonomous College, Mumbai, India 400019.*
[2]*High Pressure and Synchrotron Radiation Physics Division, Bhabha Atomic Research Centre, Mumbai, India 400085.*
[3]*Homi Bhabha National Institute, Mumbai, India 400085.*

Herein, we investigate the interaction mechanism of uranium (U) and its compounds with γ-Graphyne (γG) and N-doped γG using a pseudo-electron- and all-electron-based density functional theory (DFT) approach. Carbon nanostructures like fullerenes, carbon nanotubes, graphene and their functionalized structures have become an interesting field of study in theoretical and experimental fields.[1] γG is a structural analogue of graphene having a layered structure containing hexagonal rings joined together by acetylenic linkages and hence provides more flexibility than graphene.[2,3]

System	Binding Energy (eV)			
	GGA	**GGA +U(U=2.05)**	**HSE06**	**WEIN2k**
γG+U	-5.235	-5.338	-5.4255	in progress
NγG+U	-5.5454	-5.6365	-4.65	in progress
γG+UN	-3.683	-3.817	-2.732	in progress
NγG+UN	-4.006	-4.1255	-3.023	in progress
γG+UCl$_3$	-1.82			in progress
NγG+UCl$_3$	-1.99			in progress

Table 1: Binding energy of U and U stable molecules with γG and NγG

We have computed the binding energies for the pseudoelectron-based DFT using the plane-wave code, VASP (Vienna ab initio simulation package) employing the generalized gradient approximation (GGA-PBE). To improve on the accuracy of the GGA-PBE functional, we added the Hubbard correction term which accounts for the Coulombic interactions in localized electrons via the *U* term for the strongly correlated *d* and *f* electronic states. We used a hybrid functional (HSE06) which incorporates a part of the exact Hartree–Fock exchange interactions and compare all the binding energy values in Table 1. The interaction of NγG with U is more negative as compared to γG indicating the process to be energetically favorable. Urea-functionalized γG shows an improved binding with U as compared to γG. We have studied the mechanism of interaction via density of states and charge transfer studies. An all-electron DFT code, such as WEIN2k,[4,5] can more accurately predict the electronic behaviour of strongly correlated systems. Thus, the U *f* electron contributions to its interaction with γG and NγG can be explored. These calculations are in progress.

References:
1. Z. Li, F. Chen, L. Yuan, Y. Liu, Y. Zhao, Z. Chai and W. Shi, *Chemical Engineering Journal*, 2012, **210**, 539–546.
2. J. Kang, J. Li, F. Wu, S.-S. Li and J.-B. Xia, *J. Phys. Chem. C*, 2011, **115**, 20466–20470.
3. M. Singh, A. Shukla, and B. Chakraborty, *Int. J. Hydrog. Energy*, 2023, **96**, 37834–37846.
4. P. Blaha, K. Schwarz, G. K. Madsen, D. Kvasnicka, and J. Luitz, 2001, **60**(1).
5. P. Blaha, K. Schwarz, F. Tran, R. Laskowski, G. K. H. Madsen and L. D. Marks, J. Chem. Phys., 2020, **152**, 074101.

First-principles phonon calculations of thermal expansion path of Fe₂Mo Laves phase

Dmitry Vasilyev

Baikov Institute of Metallurgy and Materials Science of RAS, Moscow, Russia

dvasilyev@imet.ac.ru ; vasilyev-d@yandex.ru

The thermodynamic properties of solids are currently modeled from first-principles calculations using the quasi-harmonic approximation (QHA). The free energy of a solid can be expressed in terms of QHA as a sum of the total energy $E_{tot}(V)$ obtained from first-principal calculations at T = 0K, the electronic $F_{el}(V,T)$, vibrational $F_{vib}(V,T)$ and magnetic $F_{mag}(V,T)$ free energies. The vibrational energy, in turn, can be obtained either using the Debye–Grüneisen method or using the phonon calculations, as was done in [1, 2].

The vibrational energies obtained along the thermal expansion path of the C14 Fe₂Mo Laves phase calculated using the Debye model [1] and using phonons [2] are shown in Figure 1. The calculation results show that the difference in the energy obtained by these two methods, neglecting the difference δ in calculated zero oscillations, corresponds to the entropy of the magnetic moments of atoms distributed on different sublattices of Fe₂Mo compound. This can be expressed as:

$$F_{phonon}(V,T) = F_{Debye}(V,T) - T \cdot S_{mag}(V,T) - \delta$$

Therefore, when using the Debye model, it is necessary to take into account the magnetic entropy for a correct description of the thermodynamic properties.
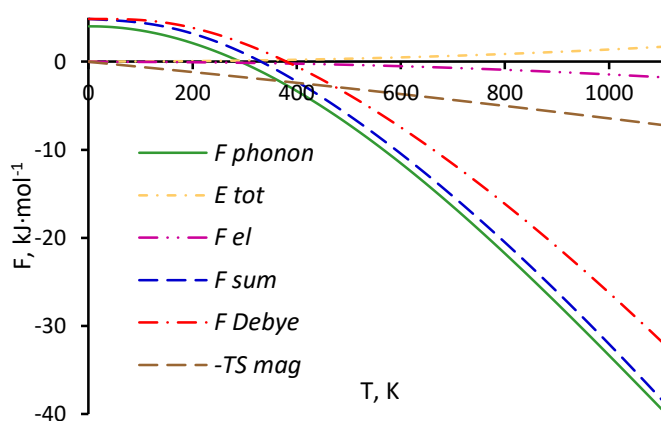

Figure 1. Free energy (*F phonon*) obtained as a sum of the total, electronic and vibrational energies calculated using *ab initio* based phonon calculations along the thermal expansion path of Fe₂Mo; free energy (*Fsum*) calculated as a sum of the total, electronic, magnetic entropy (-*T·Smag*) and vibration energy (*FDebye*) reported in [1].

1. D. Vasilyev, A new method for calculating the thermodynamic and physical properties of compounds: Application to Laves phase Fe2Mo, Physica B: Condensed Matter 621 (2021) 413307.
2. D. Vasilyev, Comparison of thermal expansion path of the Fe2Mo Laves phase calculated using the DFT-based phonon and Debye-Gruneisen approaches, Materials Today Communications 35 (2023) 105550.

Inducing out-of-plane magnetocrystalline anisotropy by chemical doping in 2D multiferroic CuCrP$_2$S$_6$

Anita Yadav[1], **Natasa Stojic**[1], **and Nadia Binggeli**[1]

[1]*Abdus Salam International Centre for Theoretical Physics, ICTP, Strada Costiera 11, 34151 Trieste, Italy*

The rapid progress in the field of electronics necessitates the exploration of novel materials with enhanced functionalities to meet the demands of emerging technologies. In recent years, multiferroics [1, 2, 3, 4] have attracted significant interest owing to the coexistence of multiple ferroic phases, including ferromagnetic, ferroelectric, and ferroelastic properties. The coupling of spontaneous electric polarization with magnetism enables new technologies with improved performance in a wide range of applications, such as memory devices, sensors, and spintronics. In this work, we performed first-principles calculations to investigate the modulation of magnetic anisotropy (MCA) in 2D multiferroic CuCrP$_2$S$_6$ by introducing a non-magnetic dopant, Indium. Our results unveil a notable transition from in-plane to out-of-plane MCA as the concentration of Indium in the mixed CuCr$_{1-x}$In$_x$P$_2$S$_6$ increases. This effect is attributed to the change in the lattice structure and the hybridization of the in-plane d-orbitals of the Chromium atom in the presence of a heavier and non-magnetic element, such as Indium, which alters the magnetic interactions and leads to a reorientation of the magnetization direction. These findings suggest a practical avenue for tailoring the magnetic behavior of 2D multiferroics, thus opening new possibilities for advanced device applications.

[1] W. Eerenstein, N. D. Mathur, and J. F. Scott, Nature **442**, 759 (2006).

[2] H. Schmid, Ferroelectrics **162**, 317 (1994).

[3] S.-W. Cheong and M. Mostovoy, Nature Materials **6**, 13 (2007).

[4] R. Ramesh and N. A. Spaldin, Nature Materials **6**, 21 (2007).

Elucidating the chemical and structural variability in the efficiency of band edge optical transitions of 2D monolayer materials

A. F. Gomez-Bastidas[1], **K. Sriram**[1], **A. C. Garcia-Castro**[2], **and O. Rubel**[1]

[1] *Department of Materials Science and Engineering, McMaster University, 1280 Main Street West, Hamilton, Ontario L8S 4L8, Canada*

[2] *School of Physics, Universidad Industrial de Santander, Carrera 27 Calle 09, Bucaramanga, Santander 680002, Colombia*

We performed a theoretical and computational analysis pursuing the following main goals: (i) to discern and rank 2D monolayer materials with potential as optical emitters, and (ii) to deepen comprehension of the physical and chemical factors influencing the oscillator strength of these materials. To do so, we employed the density-functional theory (DFT) [1, 2] calculations and theoretical analyses on a wide range of 2D monolayer materials showing direct band gap energies. As such, we focused particularly on optical matrix elements between band edges. We elucidated cases where the optical matrix elements vanish, *i.e.* forbidden optical transitions due to selection rules from group theory. Nevertheless, many 2D materials exhibit optical transitions between conduction band edge (CBE) and valence band edge (VBE) that are not forbidden by group theory. In such cases, the momentum matrix elements vary from nearly 0 up to 0.6 at. u. depending on the specific structure and composition. We also observed that, for comparison, the most prominent group III-V bulk semiconductors have the optical matrix elements on the order of 1 at. u. This suggests potential advantages of such materials to be employed as candidates for 2D materials optical emitters.
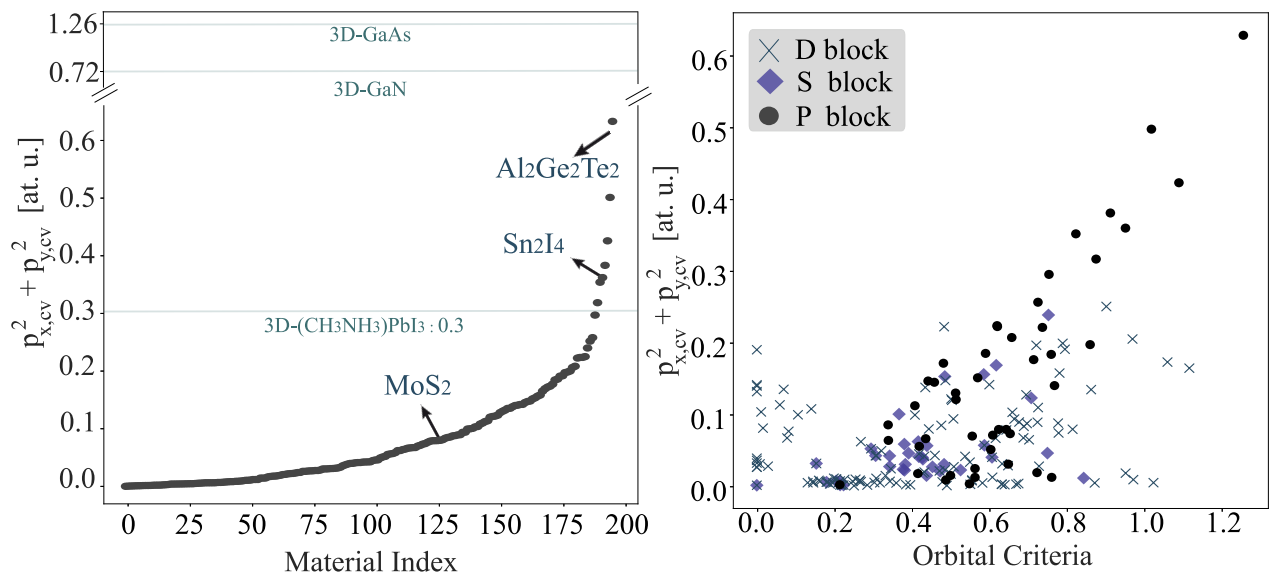

Figure 1: The results of the computed In-plane momentum matrix elements between VBE and CBE a) in ascending order, where a variability from 0 to 0.6 at. u. can be evidenced; values from well known 3D materials are presented for comparison. b) In-plane momentum matrix elements plotted versus the criteria based on the atomic optical transition selection rules between VBE and CBE. The materials with solely D-block elements present the higher values and predictability.

[1] P. Hohenberg, W. Kohn, J. Phys. Rev. **136**, B864 (1964).
[2] W. Kohn and L. J. Sham, Phys. Rev. **140**, A1133 (1965).
[3] S. Haastrup, et. al., 2D Mater. **5**, 042002 (2018).